PREDICTION OF HEAT TRANSFER AND CHAR LAYER THICKNESS IN ROCKET NOZZLE LINER

A Thesis Submitted
In Partial Fulfilment of the Requirements
for the Degree of
MASTER OF TECHNOLOGY

by

JAYACHANDRAN T.

to the

DEPARTMENT OF AERONAUTICAL ENGINEERING
INDIAN INSTITUTE OF TECHNOLOGY, KANPUR

AUGUST, 1983

Dedicated to

my parents

ACKNOWLEDGEMENTS

It is with deep sense of gratitude that I express my indebtedness to my guide, Dr. O.P. Sharma for his exemplary guidance and encouragement throughout the course of this work. I have been benefitted immensely from the discussions, I had with him from the time the project was conceived, through its execution upto the time of thesis completion.

I am also grateful to Dr. E.S. Reddy for his valuable suggestions.

I should like to record my thanks to Mr. C.M. Abraham for his excellent typing.

Thanks are also due to my friends Thomas, Sarat and Ramachandran for their painstaking efforts in bringing this thesis to its present form and making my stay in IIT Kanpur a memorable one.

Jayachandran, T.

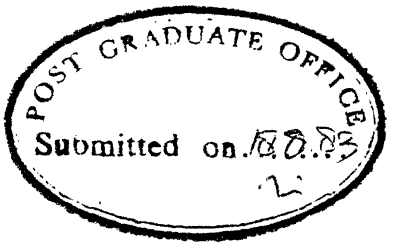

CERTIFICATE

This is to certify that the work for the thesis entitled, 'PREDICTION OF HEAT TRANSFER AND CHAR LAYER THICKNESS IN ROCKET NOZZLE LINER', has been carried out by Shri T. Jayachandran under my supervision and that it has not been submitted elsewhere for a degree.

O P Sharma

(Dr. O.P. SHARMA)
Professor
Department of Aeronautical Engineering
Indian Institute of Technology
Kanpur.

CONTENTS

LIST OF FIGURES

TABLE OF CONTENTS

NOMENCLATURE

A	Local cross-sectional flow area; pre-exponential term in Arrhenius equation
A_o^+	constant
b_1, b_2	blowing parameters
C^*	characteristic velocity
C_f	skin friction coefficient
C_p	specific heat at constant pressure
D	local diameter; damping function
d	penetration depth
E/R	characteristic activation temperature
h	enthalpy; heat transfer coefficient
k	thermal conductivity
K_m	mixing length constant
m	exponent of temperature dependence of viscosity
M	Mach number
u	density ratio exponent, Arrhenius equation
p	pressure
p^+	pressure gradient parameters - $\frac{dp}{dx} \frac{\nu_e}{\rho_e u_\tau^3}$
P_r	Prandtl number
$\dot{q}$	heat flux rate
Q_p	heat of pyrolysis
r_c	radius of curvature at the throat
r	nozzle radius at any section
R	recovery factor

S_t Stanton number $\dfrac{\dot{q}_w}{(h_{t,ad}-h_w)\,\rho_e u_e}$

t time

T temperature

u^+ dimensionless velocity u/u_τ

u velocity component tangential to the wall

u_τ friction velocity $(\tau_w/\rho_w)^{\frac{1}{2}}$

v velocity component normal to the wall

x distance along the wall

X Char depth

y distance normal to the wall

y^+ dimensionless normal distance $\dfrac{\rho_w u_\tau y}{\mu_w}$

Z axial distance from throat

α nozzle half angle

γ ratio of specific heats

δ^* displacement thickness $\equiv \int_0^\infty (1-\frac{\rho u}{\rho_e u_e})dy$

θ momentum thickness $\equiv \int_0^\infty \frac{\rho u}{\rho_e u_e}(1-\frac{u}{u_e})\,dy$

$\mathcal{K}$ thermal diffusivity

μ dynamic viscosity

ν kinematic viscosity

ρ density

τ shear stress

φ dimensionless velocity $= u/u_e$

ψ energy thickness $\equiv \int_0^\infty \frac{\rho u}{\rho_e u_e} (1-\xi)dy$

ω viscous transformation exponent

ξ dimensionless enthalpy $\frac{h_t - h_{t,w}}{h_{t,o} - h_{t,w}}$

Subscripts

ad	adiabatic wall
c	char
e	free stream
l	virgin material
o	stagnation condition
p	pyrolysis
w	wall
t	total

Superscripts

o	initial conditions
*	throat conditions

ABSTRACT

The determination of heat transfer and char layer thickness in a composite liner of a rocket nozzle has been done by using approximate methods. The compressible turbulent boundary layer flow along the nozzle wall is analyzed to obtain heat transfer rate by using modified Van Driest's eddy diffusivity model for velocity profile, quadratic relationship between the velocity and the total enthalpy as well as the integral momentum and enthalpy equations. Assuming quasi-steady situation the char layer thickness is calculated by using a simplified procedure for approximate solution of heat transfer problem with a moving interface. Comparison of the calculated results with some experimental data and other related theoretical results has been done.

CHAPTER 1

INTRODUCTION

1.1 GENERAL BACKGROUND

During the operation of a chemical rocket motor, heat is transmitted to all the parts which are exposed to the combustion products, such as, solid-propellant grain, liquid-propellant injector face, chamber and nozzle walls. The determination of heat transfer rate and the choice of an appropriate thermal protection method is essential for the design and development of rocket motors. Here we will be concerned, only with the heat transfer and cooling in a rocket nozzle. The objective is to protect the nozzle walls especially the critical hot regions so that the performance of the rocket motor follows the desired behaviour.

Inadequate thermal protection of a nozzle may lead to the breakdown/unpredictable rocket motor operation, such as, in the following situations :

1. The wall temperature exceeds the value at which the material is readily melted or oxidized. The local loss of material weakens the wall so that it is no longer able to withstand the imposed load.

2. An uneven erosion of the throat region takes place resulting in mis-alignment of the thrust vector.

Some of the cooling methods used in rocket nozzles are : 1) Insulation cooling, 2) Heat sink cooling, 3) Transpiration cooling, 4) Regenerative cooling, and 5) Ablative cooling. Some times a combination of some of these methods has also been employed.

For solid propellant rocket motors,only a few of the above-mentioned methods like insulation cooling and ablative cooling have been found useful. The ablative cooling has been successfully used in large booster rockets and the present study deals only in this method of cooling.

In ablative cooling, the inner surface of the nozzle walls is lined with a composite material consisting of layers of woven fibres (such as silica or carbon/graphite fibres) impregnated with an organic plastic material (such as epoxy or phenolic). The liner when exposed to a high heat flux undergoes complex thermo-physical phenomena keeping the inner nozzle wall at the desired lower temp The term 'ablation' implies the occurrence of heat and mass transfer processes in which a large amount of thermal energy is expended by the loss of surface region material. A simplified schematic diagram identifying some distinguishing features for an ablative liner is shown in Fig. 1.

When the ablator surface temp. rises, the heat is transmitted into the virgin material and the organic plastic component first begins to decompose (pyrolysis zone II) producing gaseous products which diffuse outwards through the matrix of higher temp resistant fibres forming the so-called char layer (zone III). As the surface temp increases further, other chemical reactions such as evaporation or oxidation of char material set in, resulting in removal or erosion of surface material (zone IV). Aerodynamic forces as well as particle impact also contribute towards the surface erosion. Evidently the rate of char layer formation or surface regression depends upon the temp, velocity, etc. of the flow field over the ablator surface, and consequently, the ablator requirements will vary from one situation to another. In other words, large erosion rates in reentry heat shields may be desirable but not so in the case of rocket nozzle. Here the analysis is restricted to the determination of char layer thickness for a given heat transfer rate by using a highly simplified approach. Before giving the details of the present analysis, the past literature relevant to the topic is reviewed next.

1.2 REVIEW OF PAST CONTRIBUTIONS

The phenomena associated with the ablative cooling in rocketry has been extensively studied for the past two decades. The analysis of the problem involves determination of the heat flux at the liner surface exposed to hot

gases flowing over it and of the effect of various thermo-physical process occurring inside the liner material. Most of the investigations usually deal with only one part of the problem, that is, either the heat transfer rate or the degradation of the liner, in details by making use of the available experimental or theoretical results for the other part.

Some of the earliest investigations for the prediction of heat transfer rate from the combustion products to the rocket nozzle walls have been done and reviewed by Bartz [1]. Using integral method and 1/7th power distributions of velocity and temperature in terms of certain boundary layer shape parameters, Bartz obtained the following expression for the local heat transfer coefficient.

$$h = \left[\frac{0.026}{D^{*0.2}} \left(\frac{\mu_o^{0.2} c_p}{P_r^{0.6}}\right)\left(\frac{P_o}{C^*}\right)^{0.8} \left(\frac{D^*}{r_c}\right)^{0.1}\right]\left(\frac{A^*}{A}\right)^{0.9} \sigma \qquad (1.1)$$

where

$$\sigma = \frac{1}{\left[\frac{1}{2}\left(\frac{T_w}{T_o}\right)\left(1+\frac{\gamma-1}{2} M_e^2\right)+\frac{1}{2}\right]^{0.8-(m/5)} \left[1+\frac{\gamma-1}{2} M_e^2\right]^{m/5}}$$

The evaluation of the constant 0.026 as well as the dependence on the wall temperature was achieved by comparing the calculated results with the available experimental data for both heated air and rocket thrust chambers. Bartz

expression has been widely used because of its simplicity and has been in general found to over-estimate the heating rate.

During the past decade or so, substantial progress has been achieved in the description of compressible turbulent boundary layer flows with pressure gradients and heat as well as mass transfer due to improved experimental and theoretical/numerical techniques [2,3]. More elaborate methods of predicting heat transfer rates make use of the semi-empirical models for turbulent transport coefficients appearing in governing differential conservation equations. The differential methods involve excessive amount of numerical computation on a digital computer, and complexity of the solution increases enormously, when coupled with the phenomena occurring in the liner. It is therefore found worthwhile to devise approximate methods for predicting rapidly but reasonably correct heat transfer rates into converging-diverging nozzles.

Recently, Mastanaiah [4] reported an approximate method based on the integral equations and the eddy diffusivity model due to Van Driest and Cebecci [3] and it is claimed that the heat transfer results are better than those predicted by Bartz expression. This method has been found useful in the present investigation and the details are described in Chapter 2.

The thermo-chemical response of composite liners exposed to some heating rate has been dealt with in various ways. Sutton [5] has recently reviewed the initial development of ablative thermal protection systems. A few experiments conducted under controlled conditions provide empirical expressions for the degradation of liners which are found useful in design calculations but their range of applicability is rather limited. On the other hand, detailed investigations involving elaborate computer programs are available which attempt to deal with the problem in the most general manner possible by considering the non-equilibrium chemically-reacting boundary layer flow coupled with the chemical-kinetic-controlled heat transfer processes in the Charring ablater [6,7]. In view of the complex chemistry of the decomposition of composite materials, the development of new materials, the lack of accurate knowledge of the thermo-physical properties at the operating conditions and large computer time required for iterative cycles to achieve coupling, it is useful to devise quick and approximate solutions. Goodman [8] employed integral method to solve the heat transfer problem in the composite heat shield for a given heat flux, and has also reviewed other related investigations.

The classical problem of heat transfer with phase change finds an interesting application in the case, where different kinds of techniques have been employed to obtain approximate solutions. Newmann [9] obtained an analytic solution for a phase change problem with constant surface temp Various related problems with specified heat flux have been discussed by Boley [10] and more recently by Zien [11,12]. Here it has been found more convenient to use the approximate method of solution, for time-dependent surface temperature by Sharma et al. [13]. The details of the method are discussed in Chapter 2.

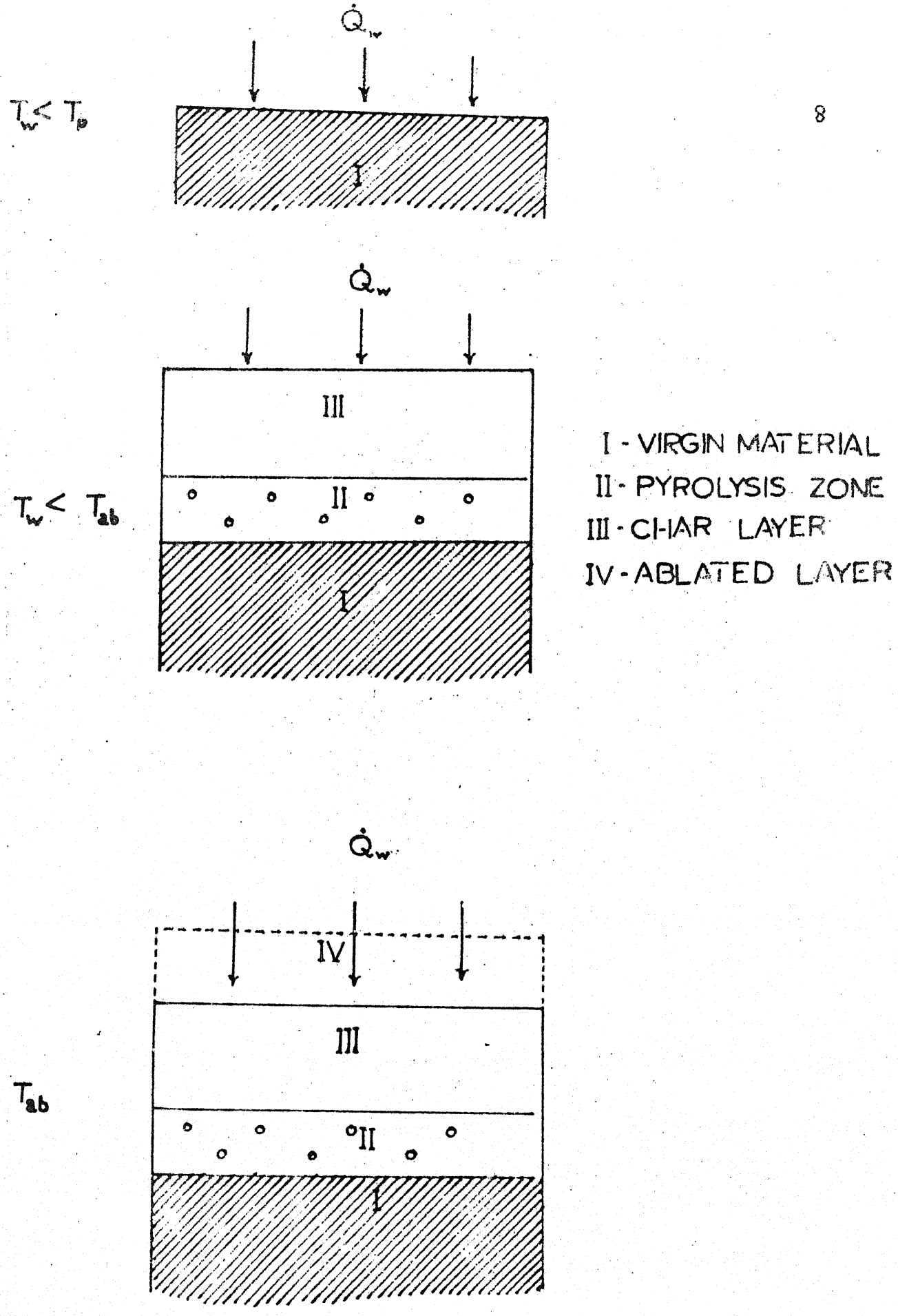

FIG: 1 SCHEMATIC DIAGRAM FOR A CHARRING ABLATOR

CHAPTER 2

FORMULATION AND METHOD OF SOLUTION

2.1 PHYSICAL MODEL

The propellantsin a rocket motor when ignited produce hot combustion products which are then accelerated through a converging-diverging nozzle to produce thrust. After a very short initial transient period, some constant stagnation conditions of the gaseous products exist in the chamber and the flow through the nozzle remains chocked. The flow field in the nozzle is assumed to be steady and is analyzed by considering one-dimensional, inviscid 'core' (or main) flow along with the turbulent boundary layer approximation over the nozzle walls (see Fig. 2). The multi-component nature of the flow has been ignored, and an approximate method of solution as described in the next section has been employed for the turbulent boundary layer flow.

The passage of hot gases over the nozzle wall transmits heat into the composite liner. Each composite liner has a threshold temperature at which significant decomposition or pyrolysis begins to take place. The pre-pyrolysis time, that is, the time taken for the liner surface to attain the pyrolysis temperature, is usually very low. As the surface

temperature of the liner increases further, the temperature of the inner layers of the liner rises and therefore pyrolysis sets in them,resulting in the formation of a char layer. The gaseous products due to pyrolysis diffuse outwards through the char layer, and thereby reducing the heat transfer from the hot propellant gases. Assuming that the pyrolysis is restricted to a very thin zone, the complex thermo-physical processes occurring within the composite liner have been described simply as an approximate unsteady heat transfer problem with a char front moving into virgin material (see Fig. 3) and an approximate method described later has been used to solve it.

2.2 MATHEMATICAL FORMULATION AND ANALYSIS

The mathematical formulation of the problem consists of essentially three main parts, namely, the 'core' flow in the nozzle, the compressible turbulent boundary layer flow on the nozzle walls, and the heat transfer phenomenon in the composite liner. Of course, each is coupled to the other through appropriate interface matching conditions. It is reasonable to assume a quasi-steady situation in the sense that the high speed nozzle flow adjusts itself quickly to the changes at the surface of the composite liner in which heat transfer process is unsteady. The underlying assumptions and the governing equations for each part are described below separately.

A. 'Core' Flow :

The main flow in the nozzle is assumed to be steady, one-dimensional and inviscid, and the hot gases are assumed to obey ideal gas equation of state with a suitable gas constant as well as to have a constant average specific heat. Under these assumptions the governing equations for the 'core' flow may be expressed as follows (see, for example, Shapiro [14]) :

Mass conservation : $\rho_e u_e A = \text{const} = \dot{m}$ (2.1)

Momentum conservation : $\rho_e u_e \left(\frac{du_e}{dx}\right) = - \left(\frac{dp_e}{dx}\right)$ (2.2)

Energy conservation : $C_p T_e + \frac{1}{2} u_e^2 = \text{const} = C_p T_o$ (2.3)

Equation of state : $p_e = \rho_e R T_e$ (2.4)

The symbols have been defined under the heading 'Nomenclature'. These equations can be easily integrated to obtain the following results :

$$\frac{A}{A^*} = \frac{1}{M_e} \left[\frac{2}{\gamma+1} \left(1 + \frac{\gamma-1}{2} M_e^2\right)\right]^{\left[(\gamma+1)/2(\gamma-1)\right]} \quad (2.5)$$

$$\frac{T_o}{T_e} = 1 + \left(\frac{\gamma-1}{2}\right) M_e^2 \quad (2.6)$$

$$\frac{p_o}{p_e} = \left(T_o/T_e\right)^{(\gamma/\gamma-1)} \quad (2.7)$$

B. Turbulent Boundary Layer Flow :

For the operating conditions of a typical rocket motor, there will exist compressible turbulent boundary layer along the nozzle wall. Several approaches have been developed over the years for analysing turbulent boundary layer flows. In order to avoid the complexity of solving non-linear, partial differential form of the turbulent boundary layer equations, the so-called 'integral method' based on the 'integral' forms of these equations have been found useful especially to predict the wall parameters. The integral momentum and energy equations for a compressible turbulent boundary layer in axisymmetric flow can be easily derived (see, for example, Bartz [1]) and expressed respectively as follows :

$$\left(\frac{d\theta}{dx}\right) + \theta\left\{\left(2+\frac{\delta^*}{\theta} - M_e^2\right)\frac{1}{u_e}\left(\frac{du_e}{dx}\right) + \frac{1}{r}\left(\frac{dr}{dx}\right)\right\} = \tfrac{1}{2}\, C_f \qquad (2.8)$$

$$\left(\frac{d\gamma}{dx}\right) + \gamma\,\frac{d}{dx}\left\{\log_e\left[\rho_e u_e (h_{t,o}-h_{t,w})r\right]\right\} = \zeta_{ad,w}\cdot St \qquad (2.9)$$

From the equations governing the 'core' flow, eqns. (2.1) to (2.4), it can be readily shown that

$$\frac{1}{u_e}\left(\frac{du_e}{dx}\right) = \left[\frac{1}{M_e\left(1+\frac{\gamma-1}{2}M_e^2\right)}\right]\left(\frac{dM_e}{dx}\right) \qquad (2.10)$$

$$\left(\frac{1}{\rho_e u_e}\right)\left[\frac{d(\rho_e u_e)}{dx}\right] = \left[\frac{1-M_e^2}{M_e\left(1+\frac{\gamma-1}{2}M_e^2\right)}\right]\left(\frac{dM_e}{dx}\right) \qquad (2.11)$$

Equations (2.8) and (2.9) can be used to determine the Skin friction coefficient (C_f) and the Stanton number (St) provided the velocity and the temperature profiles become known. Past experience has shown that the wall parameters can be predicted to a reasonable accuracy by using approximate profiles such as in the pioneering work due to Bartz [1].

Here, in order to obtain approximate velocity and temperature profiles, the more recently acquired knowledge in describing the structure of turbulent boundary layer flows has been incorporated as suggested by Mastanaiah [4]. The earliest models for the phenomenological description of the coefficient of momentum transport or the so-called Reynolds stress were proposed by Prandtl and Boussinesq in terms of mixing length and eddy viscosity parameters. Van Driest [15] extended its applicability over the entire boundary layer for flows with negligible pressure gradient and zero mass transfer. Cebecci [3] generalized it to flows with pressure gradient mass transfer and heat transfer. In terms of dimensionless quantities, the generalized eddy viscosity expression can be written as

$$\frac{du^+}{dy^+} = \frac{2}{\left[\frac{\mu}{\mu_w} + \left\{\left(\frac{\mu}{\mu_w}\right)^2 + 4\left(\frac{\rho}{\rho_w}\right)(K_m y^+ D)^2\right\}^{\frac{1}{2}}\right]} \qquad (2.12)$$

where

$$D = 1-\exp(-y^+/A^+) \text{ and } A^+ = A_o^+(1-11.8P^+) \qquad (2.13)$$

In equation (2.13), A_o^+ is taken as 26, and in eqn. (2.12), K_m, the mixing length constant as 0.4 . The temperature dependence of the coefficient of viscosity is described as T^m, m being equal to 0.6. Here eqn. (2.12) has been used to determine the velocity distribution across the boundary layer.

The relationship between temperature and velocity profiles in a turbulent boundary layer along supersonic nozzle with heat transfer has been investigated by Back and Cuffel [16]. They have found that the usual Crocco-relationship is no longer valid and that the acceleration parameter plays a prominent role. Following Mastanaiah [4], a quadratic enthalpy-velocity relationship of the form given below is assumed :

$$\frac{}{} = A_1\varphi + A_2\varphi^2 \qquad (2.14)$$

where A_1 and A_2 are determined by using the boundary conditions at the wall, namely,

$$\text{At } y = o,\ u = o,\ T = T_w,\ \mu\left(\frac{\partial u}{\partial y}\right) = \tau_w,\ -k\left(\frac{\partial T}{\partial y}\right) = \dot{q}_w \qquad (2.15)$$

After some algebraic manipulations and also making use of the differential form of conservation equations for momentum and total enthalpy, it can be shown that

$$A_1 = 2P_r(St/C_f)\,\mathcal{F}_{ad,w}$$

$$A_2 = \left(\frac{1-P_r}{h_{t,o}-h_{t,w}}\right)\frac{u_e^2}{2} + \left(\frac{2A_1}{C_f^2}\right)\left(\frac{\rho_w\mu_w h_w}{\rho_e^2 u_e h_o}\right)\frac{d\log_e(M_e)}{dx} \qquad (2.16)$$

The above set of equations, namely equations (2.5), (2.8), (2.9), (2.12) and (2.14) are sufficient for the determination of skin friction coefficient and Stanton number for a known constant wall temperature.

C. Gas-Solid Interface Condition :

The heat flux into the constant-temperature nozzle-wall varies along the axis of the nozzle, and at any given station it depends upon the magnitude of the wall temperature. When the nozzle-wall is lined with a composite material, certain thermophysical processes occur at the gas-solid interface as described in the last section resulting in the coupling of turbulent boundary layer flow with the physical phenomena taking place within the composite liner. Both the surface temperature and the heat flux change with

time soon after the motor is fired. At any instant the heat flux from the gaseous phase can be expressed as

$$\dot{q}_w = h(T_{ad}-T_w) \qquad (2.17)$$

The adiabatic wall temperature can be obtained from the relation

$$T_{ad} = T_o \left[\frac{1 + \frac{\gamma-1}{2} R M_e^2}{1 + \frac{\gamma-1}{2} M_e^2}\right] \qquad (2.18)$$

where, the recovery factor, R is taken equal to $P_r^{1/3}$.

At any station on the nozzle wall, T_{ad} is constant while $\dot{q}_w$ will vary with T_w and consequently the magnitude of the heat transfer coefficient, h, will also change. The details of the coupling of the heat transfer and the decomposition of liner is discussed later.

When the pyrolysis sets in the composite liner, the heat flux at the surface is affected by the gaseous products of pyrolysis which diffuse outwards. The heat blockage due to pyrolysis is determined by using a correlation due to Fogaroli and Laganelli [17] which takes into account both Mach number and wall temperature variations but assumes very small pressure gradients. This correlation is as follows :

$$\frac{S_t}{S_t^o} = \left[1 - \frac{b_1}{b_2}\right]^{2.5} \qquad (2.19)$$

where the superscript 'o' refers to Stanton number without pyrolysis-effect and

$$b_1 = (C_{p,inj}/C_{p,g})\ [(\rho v)_w/(\rho u)_e]\ (1/St^o)$$

$$b_2 = \exp[1.676(\omega + 0.161)]$$

and

$$\omega = \frac{1}{8} M_e + (T_w/T_e)^{-1/8}$$

The mass flow rate of the pyrolysis gases, $(\rho v)_w$, is determined from the kinetic equations describing the thermal degradation reactions in the pyrolysis zone. Since most polymers degrade in a highly complex manner, semi-empirical homogeneous kinetics are normally used to describe the degradation by an Arrhenius type of equation. That is,

$$\frac{\partial \rho}{\partial t} = -A \exp(-E/RT)\ \rho_o\ \left(\frac{\rho - \rho_r}{\rho_o}\right)^n \qquad (2.20)$$

D. Heat Transfer in the Liner :

It is reasonable to assume that the temperature gradient in the transverse direction is much greater than that in the longitudinal direction. During the pre-pyrolysis period, the heat transfer in the composite liner is then governed by the unsteady one-dimensional heat conduction equation :

$$\left(\frac{\partial T_1}{\partial t}\right) = \mathcal{K}_1 \left(\frac{\partial^2 T_1}{\partial x^2}\right) \; ; \quad o < t < t_p, \quad x > o \tag{2.21}$$

subject to the boundary conditions :

$$T_1(x,o) = T_1^o \tag{2.22}$$

$$T_1(d,t) = T_1^o \tag{2.23}$$

$$-k_1 \left.\frac{\partial T_1}{\partial x}\right|_{x=o} = \dot{q}_w \tag{2.24}$$

A solution of eqns. (2.21) to (2.24) must be obtained to determine the pre-pyrolysis time. After the onset of pyrolysis, the liner can no longer be treated as made up of one substance instead it has a char portion and the remaining virgin material such that the thickness of char layer increases as the interface moves into the virgin material. Assuming constant thermal conductivities (k) and thermal diffusivities ($\mathcal{K}$) for both the char and the virgin material, the heat transfer will be governed by the following differential equations.

$$\left(\frac{\partial T_c}{\partial t}\right) = \mathcal{K}_c \left(\frac{\partial^2 T_c}{\partial x^2}\right) \quad t > t_p, \quad o < x < X \tag{2.25}$$

$$\left(\frac{\partial T_1}{\partial t}\right) = \mathcal{K}_1 \left(\frac{\partial^2 T_1}{\partial x^2}\right) \quad t > t_p, \quad X < x < d \tag{2.26}$$

subject to the boundary and interface conditions,

$$T_c(o,t) = T_w(t), \qquad t > t_p \tag{2.27}$$

$$T_1(x,t_p) = T_1'(x) \tag{2.28}$$

$$T_1(d,t) = T_1^{o} \tag{2.29}$$

$$T_c(X,t) = T_1(X,t) = T_p \tag{2.30}$$

$$k_c \frac{\partial T_c}{\partial x}\bigg|_X = k_1 \frac{\partial T_1}{\partial t}\bigg|_X + \rho Q_p \left(\frac{dX}{dt}\right) \tag{2.31}$$

Here, $T_w(t)$ in eqn. (2.27) is not known explicitly as a function of time, t and, in fact, it is responsible for the heat transfer coupling between the turbulant boundary layer and the composite liner through eqn. (2.17).

2.3 METHOD OF SOLUTION

The variables characterising the 'core' flow can be readily obtained from eqn. (2.4) to (2.7) provided the area-ratio is known at any station along the nozzle. For conical section, it can be calculated from the throat radius, the length and the convergent/divergent half angles of the section, while for contoured section, a polynomial curve, fitting the contour is found useful in determining the radius at any station. The distribution of Mach number (M_e),

pressure (P_e), temperature (T_e) of 'core' flow along the nozzle is then determined in terms of the chamber stagnation conditions P_o and T_o.

In order to deal with the turbulent boundary layer flow, experimental or assumed values of the quantities δ^* θ, ψ, C_f and S_t are needed at the entrance station of the nozzle. Using the values of C_f and S_t at the ith station of the nozzle, the velocity profile, u^+ versus y^+, can be obtained at the (i+1)th station by solving eqn. (2.12) in conjunction with eqns. (2.13) to (2.16). Since y^+ varies more rapidly compared to u^+, it is found convenient to solve for y^+ for a given step change in u^+ by a sixth order Runge-Kutta method (identified as IMSL subroutine DVERK). When the value of u approaches $0.9\ u_e$, smaller step size in u^+ is used to account for large changes in y^+ in this region, and the integration is stopped when u attains a value of $0.99\ u_e$. Thus, the velocity and temperature profiles are obtained at any station along the nozzle. Using the definitions, the displacement, momentum and energy thicknesses are then calculated at the (i+1)th station by numerical integration. Since the data points are arbitrarily spaced, a method due to Gill and Miller [18] is employed for integrating function values for arbitrarily spaced data points (identified as NAG subroutine DØ1GAF).

Having found the values of δ^*, θ and ψ at the (i+1)th station, eqn. (2.8) and (2.9) are solved simultaneously by using two-dimensional Newton-Raiphson method to get new values of C_f and S_t. The derivatives, $(d\theta/dx)$ and $d\psi/dx)$ have been approximated by forward finite difference expressions so that eqns. (2.8) and (2.9) may be expressed as follows :

$$\theta_{i+1} = \theta_i + \frac{\Delta x}{2} [f_{i+1}(\theta,x) + f_i(\theta,x)] \qquad (2.32)$$

and

$$\psi_{i+1} = \psi_i + \frac{\Delta x}{2} [g_{i+1}(\psi,x) + g_i(\psi,x)] \qquad (2.33)$$

Here f and g denote all the terms in the respective equations except the derivatives. These values of C_f and S_t are now used to calculate new velocity and temperature profiles, which, in turn, provide new values of δ^*,θ and ψ resulting in new values of C_f and S_t. In other words, the entire calculation procedure is repeated at the (i+1)th station until convergence in the values of C_f and S_t is attained with the desired accuracy.

In the case of a contoured nozzle, it is found convenient to change the independent distance co-ordinate along the nozzle axis. This can be easily done by making use of the following relationship

$$\frac{dx}{dz} = \left[1 + \left(\frac{dr}{dz}\right)^2\right]^{\frac{1}{2}} \qquad (2.34)$$

After having described the method for the determination of local heat transfer rate into the nozzle wall for a constant wall temperature, the next task is to obtain a solution of the heat transfer problem in the composite liner. For this purpose, it is assumed that the thermal penetration depth is much less than the liner thickness so that the analytic solutions for the semi-infinite geometry are employed in the analysis. An exact analytic solution of eqns. (2.21) to (2.24) for a constant heat flux may then be obtained as given below [9,12].

$$T(x,t) = \frac{\dot{q}_w}{k} \left(\frac{4\kappa t}{\pi}\right)^{\frac{1}{2}} \left(e^{-x^2/4\kappa t} - x\left(\pi/4\kappa t\right)^{\frac{1}{2}} \operatorname{erfc}\left(x/\sqrt{4\kappa t}\right)\right) \qquad (2.35)$$

The above equation provides us with estimation of time required to raise the wall temperature from some initial value to any higher temperature. It is found from the calculations that the pre-pyrolysis time is extremely short, much less than one second and therefore negligible compared to the run time of the rocket motor. Further, it may also be pointed out that since the gaseous flow does not attain steady state instantaneously, there exists an overlap of the transient period of gaseous flow and the pre-pyrolysis time.

It is, therefore, reasonable to neglect it altogether for quasi-steady analysis.

In view of the above analysis, the governing equations for char layer formation may be further simplified by setting $t_p = 0$ and $T_1'(x) = \text{const} = T_1^o$ in eqn. (2.28). An approximate solution is then obtained as a function of $T_w(t)$ following the method of Sharma et al. [13]. In this method the temperature profile in the char layer is determined by assuming an arbitrary profile which satisfies the governing equations, eqn. (2.25), and the boundary condition, eqn. (2.27), at $x = o$ as well as the interface condition, eqn. (2.31), at $x = X(t)$ resulting in the expression

$$T_c(x,t) = T_w(t) + \left[\frac{T_p - T_w(t)}{X(t)}\right]x + \frac{1}{2\mathcal{K}_c}\left(\frac{dT_w(t)}{dt}\right)[x - X(t)]x \tag{2.36}$$

The temperature gradient at $x = o$ and $x = X(t)$ can then be found from eqn. (2.36) as given below

$$\left.\frac{\partial T_c}{\partial x}\right|_{x=o} = \left[\frac{T_p - T_w(t)}{X(t)}\right] - \frac{X(t)}{2\mathcal{K}_c}\left(\frac{dT_w(t)}{dt}\right) \tag{2.37}$$

and

$$\left.\frac{\partial T_c}{\partial x}\right|_{x=X(t)} = \left[\frac{T_p - T_w(t)}{X(t)}\right] + \frac{X(t)}{2\mathcal{K}_c}\left(\frac{dT_w(t)}{dt}\right) \tag{2.38}$$

For the virgin material, an approximate estimate for the temperature gradient by using the governing equation, eqn. (2.26) and the initial condition, eqn. (2.29) is found to be

$$\left.\frac{\partial T_1}{\partial x}\right|_{x=X(t)} = -\left[\frac{T_p - T_1^o}{\sqrt{\pi \kappa_1 t}}\right] \tag{2.39}$$

Substituting for the temperature gradients from eqn. (2.38) and (2.39) in interface condition, eqn. (2.31) the movement of the char front is then given by the equation

$$\frac{dX(t)}{dt} + A\left(\frac{dT_w(t)}{dt}\right)X(t) - \frac{B[T_w(t)-T_p]}{X(t)} + \frac{C}{t^{\frac{1}{2}}} = 0 \tag{2.40}$$

where

$$A = \frac{k_c}{2\kappa_c \rho Q_p}, \quad B = \left(\frac{k_c}{Q_p \rho}\right), \quad C = \frac{k_1(T_p - T_1^o)}{\rho(\pi\kappa_1)^{\frac{1}{2}} Q_p} \tag{2.41}$$

Next, combining eqns. (2.37) and (2.17), the heat-balance condition at the gas-char interface can be expressed as

$$k_c\frac{dT_w(t)}{dt} + \frac{2\kappa_c}{X(t)}\left[\frac{k_c}{X(t)} + h\right]T_w(t) - \frac{2\kappa_c}{X(t)}\left[hT_{ad} + \frac{k_c T_p}{X(t)}\right] = 0 \tag{2.42}$$

A solution of the coupled set of ordinary, nonlinear differential equations, eqn. (2.40) and eqn. (2.42), will give the char layer thickness and the wall temperature as

time progresses. For the derivatives, the backward difference approximation is employed, that is,

$$\left.\frac{d\,X(t)}{dt}\right|_{t=t_1+\Delta t} = \frac{X(t_1+\Delta t) - X(t_1)}{\Delta t} \tag{2.43}$$

and

$$\left.\frac{dT_w(t)}{dt}\right|_{t=t_1+\Delta t} = \frac{T_w(t_1+\Delta t) - T_w(t_1)}{\Delta t} \tag{2.44}$$

subject to the conditions that

$$\text{At } t = o, \quad X = o, \quad \text{and} \quad T_w = T_1^o \tag{2.45}$$

In view of the singular nature of eqns. (2.40) and (2.42) at t = o, the numerical integrations were started by giving small increments to t and T_1^o. Further in the derivation of eqn. (2.42), the modification in the heat transfer rate, $\dot{q}_w$, due to pyrolysis-gas blockage as expressed by (2.19) is not done because the effect of blockage was found negligible. It may be pointed out that the dependence of the local heat transfer coefficient on the surface temperature is determined as described in Chapter 3, and is taken into account while solving the above set of coupled equations.

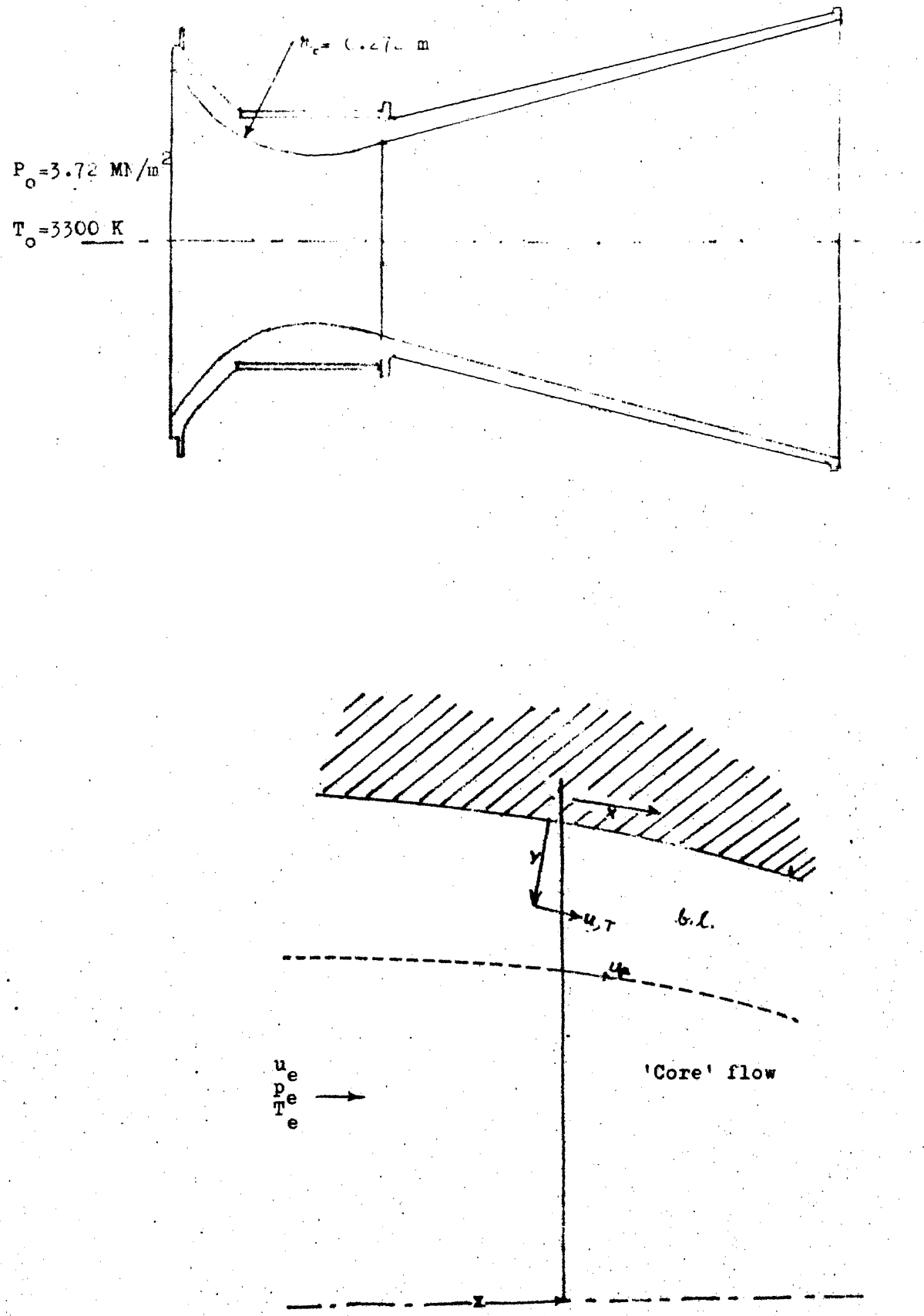

Fig. 2 Schematic diagram of rocket nozzle and the nomenclature.

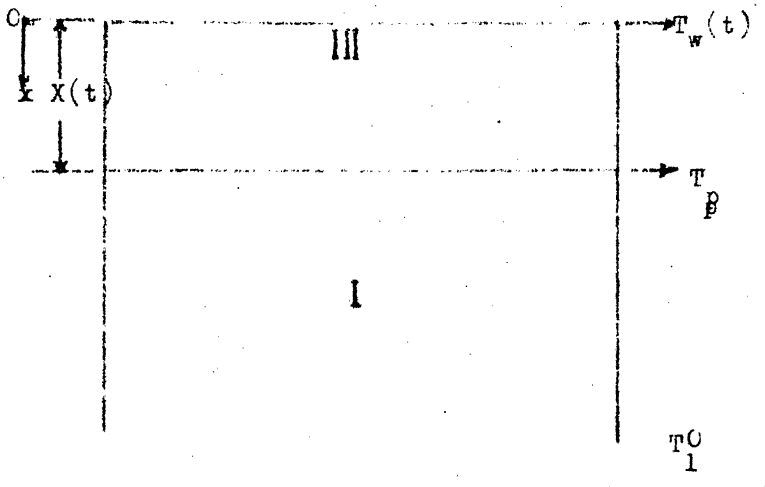

Fig. 3 Schematic diagram of a charring liner and the co-ordinate system used for its analysis.

CHAPTER 3

RESULTS, DISCUSSION AND CONCLUSIONS

3.1 RESULT AND DISCUSSIONS

The computations for predicting heat transfer rates have been done for two different situations, namely, flow of heated air in a conical nozzle and flow of combustion gases in the SLV-3 first stage nozzle. The char layer thickness calculations are done for the case of SLV-3 rocket only.

Back and Cuffel [16] measured temperature and velocity profiles in a turbulent boundary layer flow of heated air in a cooled convergent-divergent nozzle with a half angle of 10^{o} and with 10:1 contraction ratio. The nozzle throat diameter, inlet length and total length are 40.39 mm, 253 mm and 526 mm respectively. The experiment was conducted with $P_o = 1.035 \times 10^{6}$ Nm^{-2}, $T_o = 835^{o}K$ and $(T_w/T_o) = 0.5$. Under these conditions, the radiative heat transfer is found negligible. The Prandtl number is assumed constant and taken equal to 0.7. It is claimed that the heat transfer measurements are accurate to about $\pm$ 5 percent and the boundary layer thickness to within 10 to 20 percent. The comparison of the predicted heat transfer rates and other parameters with the above experimental data has been done to ascertain the accuracy of the present approximate analysis.

The computer program SARS.FOR is run using the experimental data at station 1 as the initial conditions with the interval $\Delta x = 0.02$m along the wall. Computed results showing variation of Mach number, displacement, momentum and energy thicknesses, skin friction coefficient and Stanton number along the axis of the nozzle are plotted in Fig. 4 to Fig. 8. The displacement thickness becomes negative as seen in Fig. 5 which can be attributed to the cooling of the nozzle-wall. The CPU time for one run covering the entire nozzle is found around 1.5 minutes using a step size of $\Delta U^+ = 2.0$ along the Y-direction.

A comparison of the computed Stanton number due to Mastanaiah [4], Bartz [1] (see Eq. (1.1)) and the present one with the experimental data of Back and Cuffel [16] is shown in Table 1.

The present computed results are 15 percent and about 6 percent higher than the measured values of Stanton number in the convergent and divergent sections of the nozzle respectively. The results based on Bartz closed-form approximation are much higher than the measured values. Improvement of present results as compared to those due to Mastanaiah may be attributed to the use of more accurate method of solving differential equation as well as numerical integration.

The comparison of other computed flow parameters like δ^*, θ, ψ and C_f with those of Back and Cuffel [16] is given in Table 2.

Unlike the case of Stanton number, the computed skin friction coefficient is lower than the experimental values in the convergent section.

After having established the level of accuracy of the present method of computing heat transfer rate, the calculations were done for the nozzle used in the first stage of SLV-3 rocket. The nozzle shape is shown in Fig. 2 having throat diameter equal to 330 mm. The stagnation pressure, stagnation temperature and the characteristic velocity are 3.728×10^6 Nm^{-2}, 3300^oK and 1.5328×10^3 mS^{-1} respectively. A cubic polynomial curve-fit is found adequate to describe the nozzle contour. Constant average specific heat, molecular weight and specific heat ratio of the combustion products equal to 1652J Kg^{-1} $^oK^{-1}$, 25 and 1.25 respectively have been used in the calculations. Prandtl number has been obtained from the following relationship :

$P_r = [4\gamma/(9\gamma-5)]$.

As pointed out in the last chapter, the initial values of δ^*, θ, ψ are necessary at the first station in order to proceed with the solutions of the governing equations along the nozzle. No experimental data was available

for SLV-3 rocket. However, it was possible to obtain solutions with arbitrarily chosen initial values of δ^*, θ, δ ψ . The trial runs indicated some dependence of the final results on the initial guess. Therefore, the initial values of δ^*, θ, and ψ were chosen such that the predicted heat transfer rate at the starting station gave values close to the one based on Bartz closed form expression. Slight variation of initial values around these chosen values had insignificant effect on the heat transfer rate.

The computer program SARS1.FOR is run using the above mentioned data for the nozzle-wall temperature equal to the decomposition temperature, 823°K of a typical phenolic [19] . Computed results showing the variation of Mach number, displacement, momentum and energy thickness, skin friction coefficient and Stanton number along the axis of the nozzle are plotted in Figs. 9 to 13. The displacement thickness remains negative throughout the nozzle (see Fig. 10) because the chosen value of (T_w/T_o) is rather low so that the boundary layer is highly cooled. The displacement thickness along the nozzle varies in accordance with the local heat transfer rate the variations in the momentum and energy thicknesses (see Figs. 11 to 12) are similar and depend upon the local heat transfer rate. The skin friction coefficient and Stanton number decrease at a rapid rate initially

and then increase slightly towards the end of the nozzle (see Fig. 13).

The local heat transfer coefficient variation along the nozzle is shown in Fig. 14 for $T_w/T_o = 0.25$. The maximum occurs slightly upstream of the throat. For the sake of comparison the result obtained from Bartz expression eqn. (1.1), is also shown in Fig. 14. It may be pointed out that Bartz expression has been derived by making the experimental data at the throat agree with the calculated results. The difference in the two predictions for the convergent section may be attributed to the lack of well established known initial conditions, however, in the divergent portion, Bartz expression predicts much higher heat transfer rates as compared to the present one. The dependence of heat flux rate on wall temperature for heated air data along the convergent and divergent sections of the nozzle is shown respectively in Figs. 15 and 16. As expected, the higher the wall temperature the lower is the heat flux rate and it is nearly linear.

The char layer thickness calculations were done at four different stations along the nozzle which were lined with either carbon phenolic or silica phenolic. The physical properties and the pyrolysis, kinetic parameters for both carbon phenolic and silica phenolic are given in Table 3.

A simple computer program CHAR.FOR is run using the data given in Table 3 starting with the nozzle wall at a certain known temperature. The effect of blocking due to the pyrolysis products on the wall heat transfer rate [see eqn. 2.19)]is found to be less than 1 percent and was therefore neglected.

The results of computations at five different stations along the nozzle showing variation of wall temperature and char thickness are shown respectively in Figs. 17 and 18. Comparison of the calculated char layer thickness with the available experimental data is shown in Table 4. The experimental values quoted within bracket are from reference No.20, where the specified stagnation pressure ~~specified which~~ is close to the one in reference 19. But the stagnation temperature is not specified, in ref. No.20.

The char thickness is found to be more for the carbon phenolic as compared to the silica phenolic for nearly the same heating rate. The comparison of the calculated thicknesses with the experimental data is better for carbon phenolic as compared to the silica phenolic. The variation of char depth in silica phenolic towards the aft-end of the nozzle is negligible which may be attributed to the nearly constant heat flux.

3.2 CONCLUSIONS

The general methods of calculating heat transfer rate and its effect on the liner materials in a converging-diverging nozzle involve extensive use of computer programming/numerical techniques as well as excessive computer time taken by the iterative procedure required for matching at the liner surface. The present approximate procedures yield reasonably accurate results when compared with the available data. The method is simple and can be extended to deal with higher heating rates involving regression of even the char layer, and for temperature-dependent thermal properties.

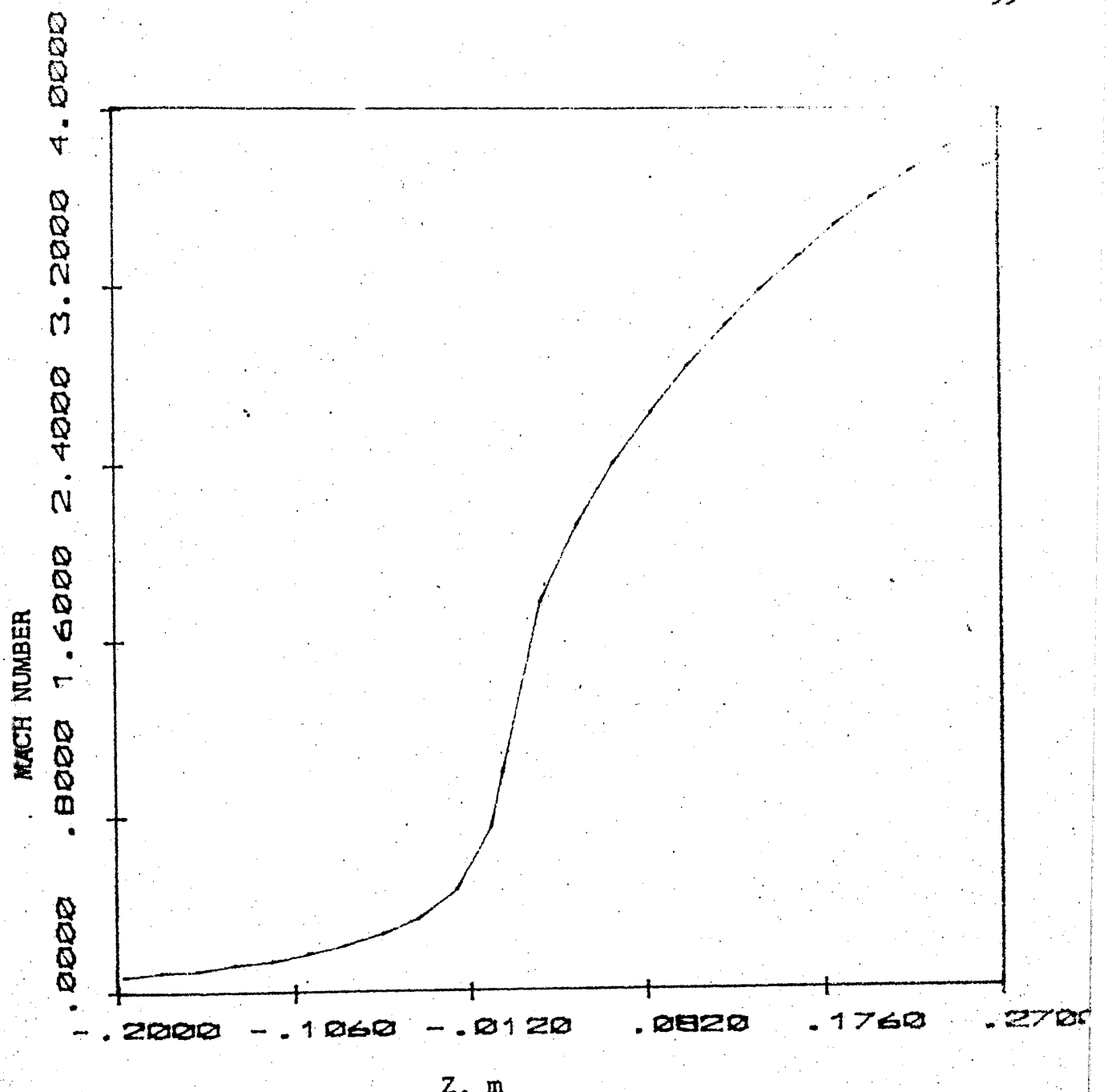

Fig. 4 Variation of the Mach number along the axis of the nozzle [16].

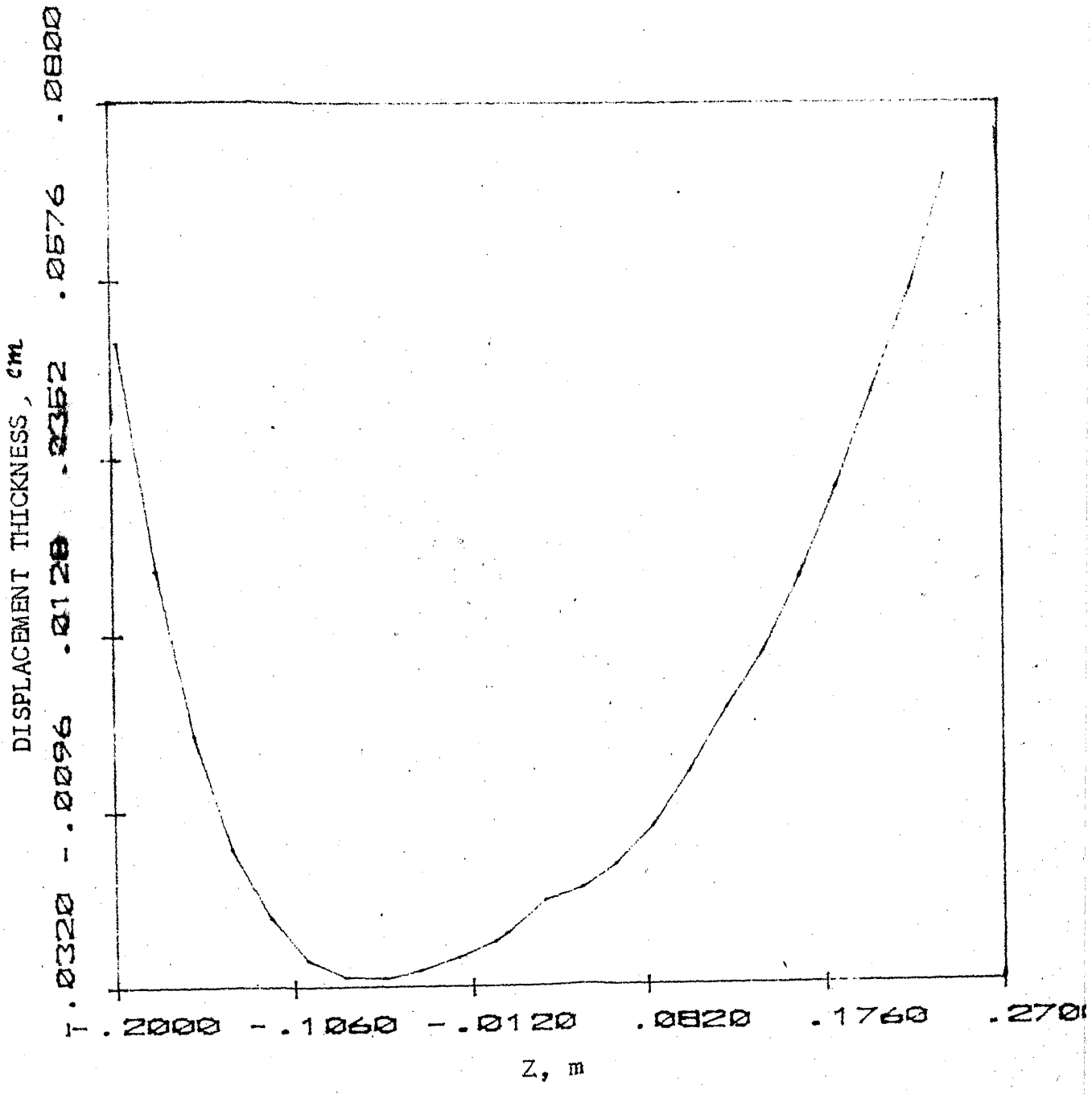

Fig. 5 Variation of Displacement thickness along the axis of the nozzle. [16].

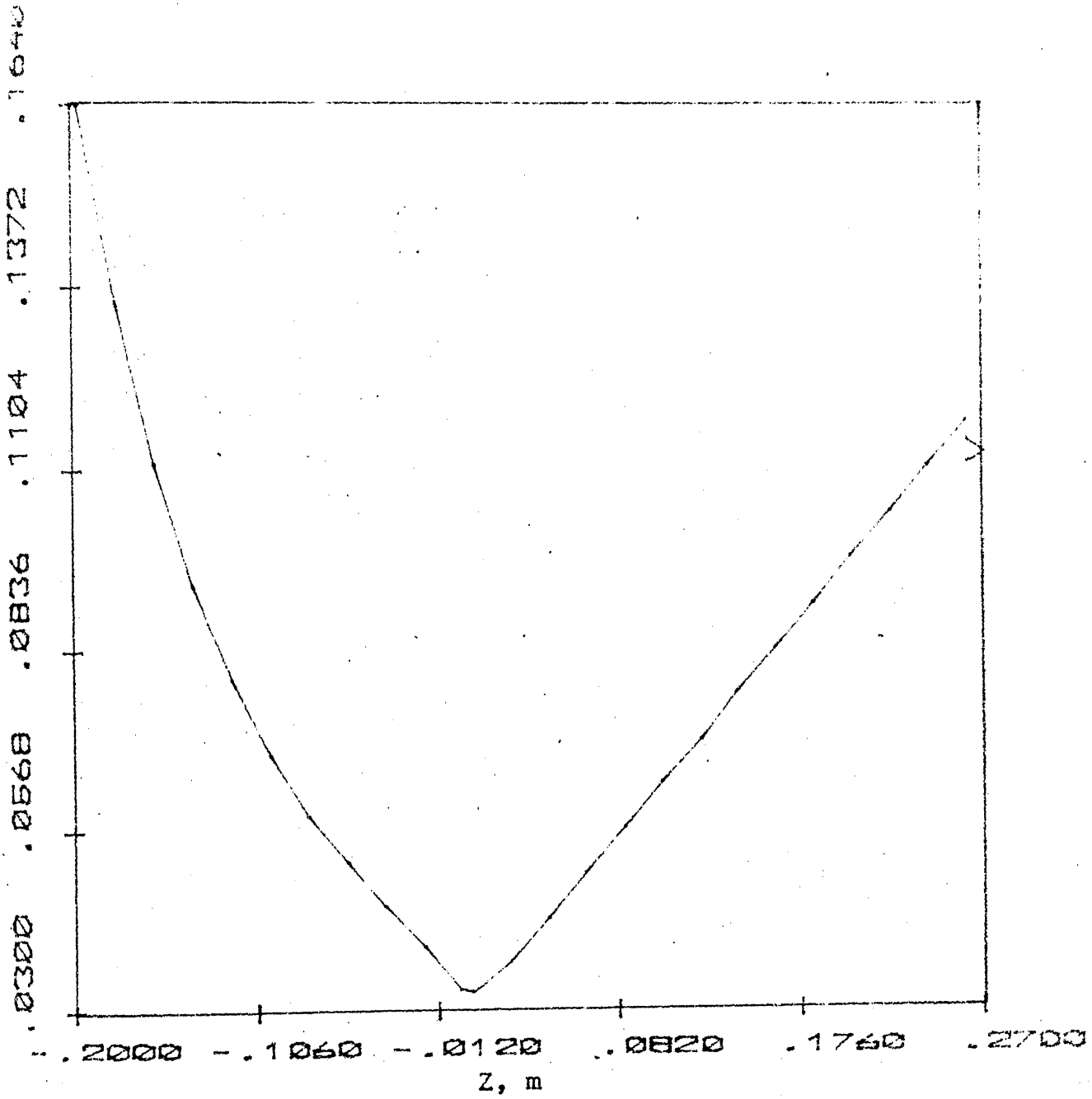

Fig. 6 Variation of Momentum thickness along the axis of the nozzle [16].

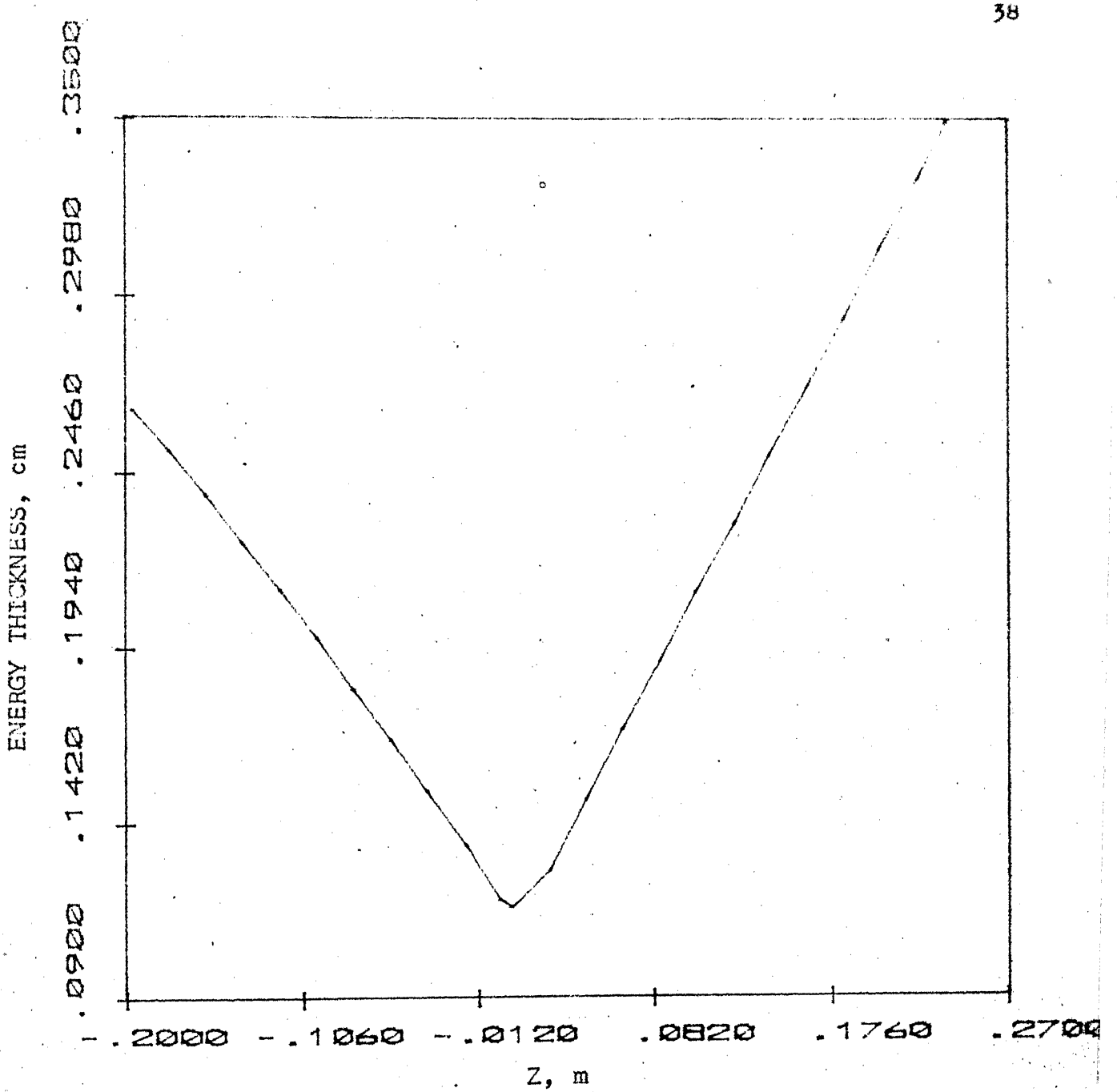

Fig. 7 Variation of energy thickness along the axis of the nozzle [16].

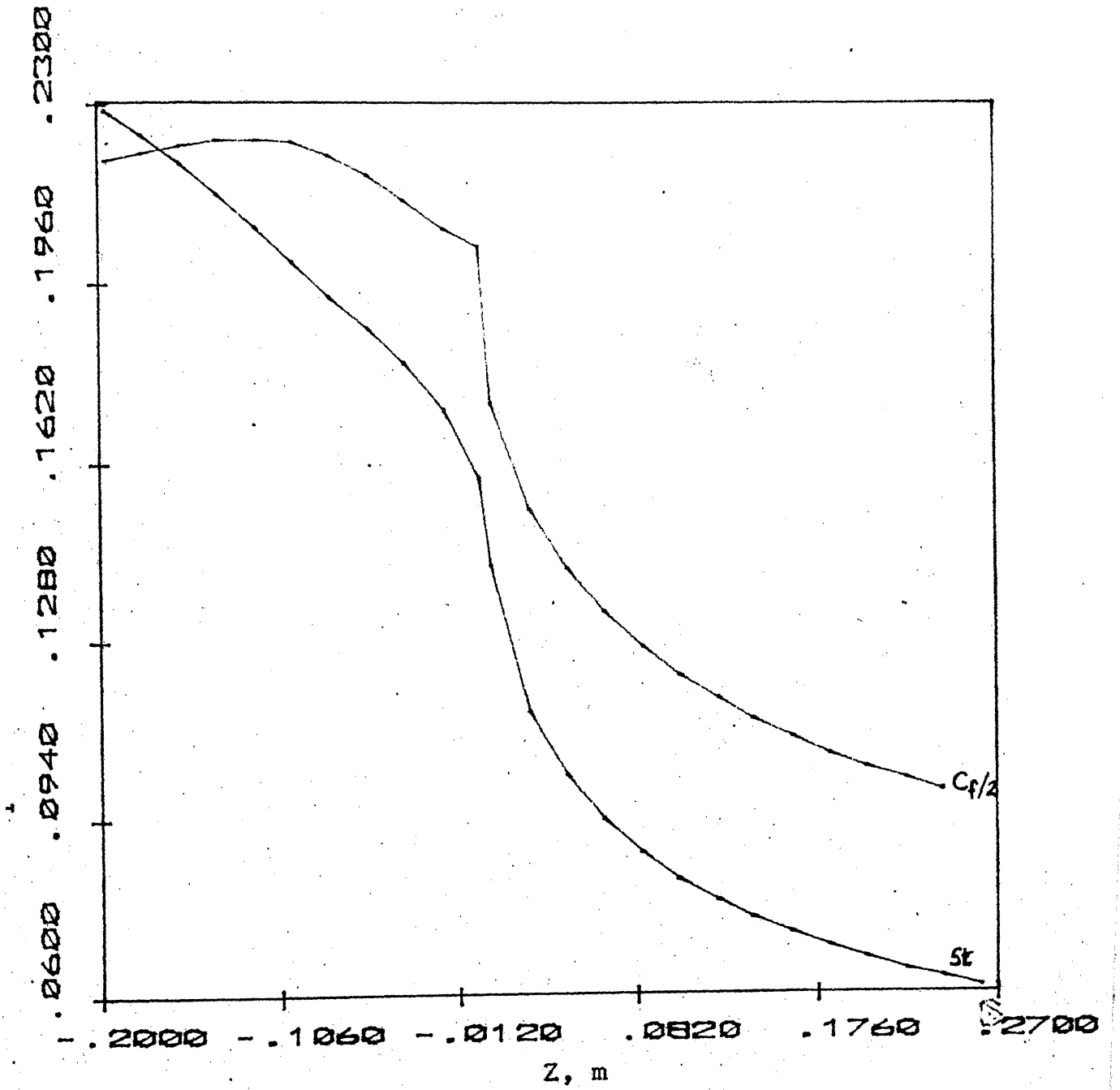

Fig. 8 Variation of Skin friction coefficient and Stanton number along the axis of the nozzle [16].

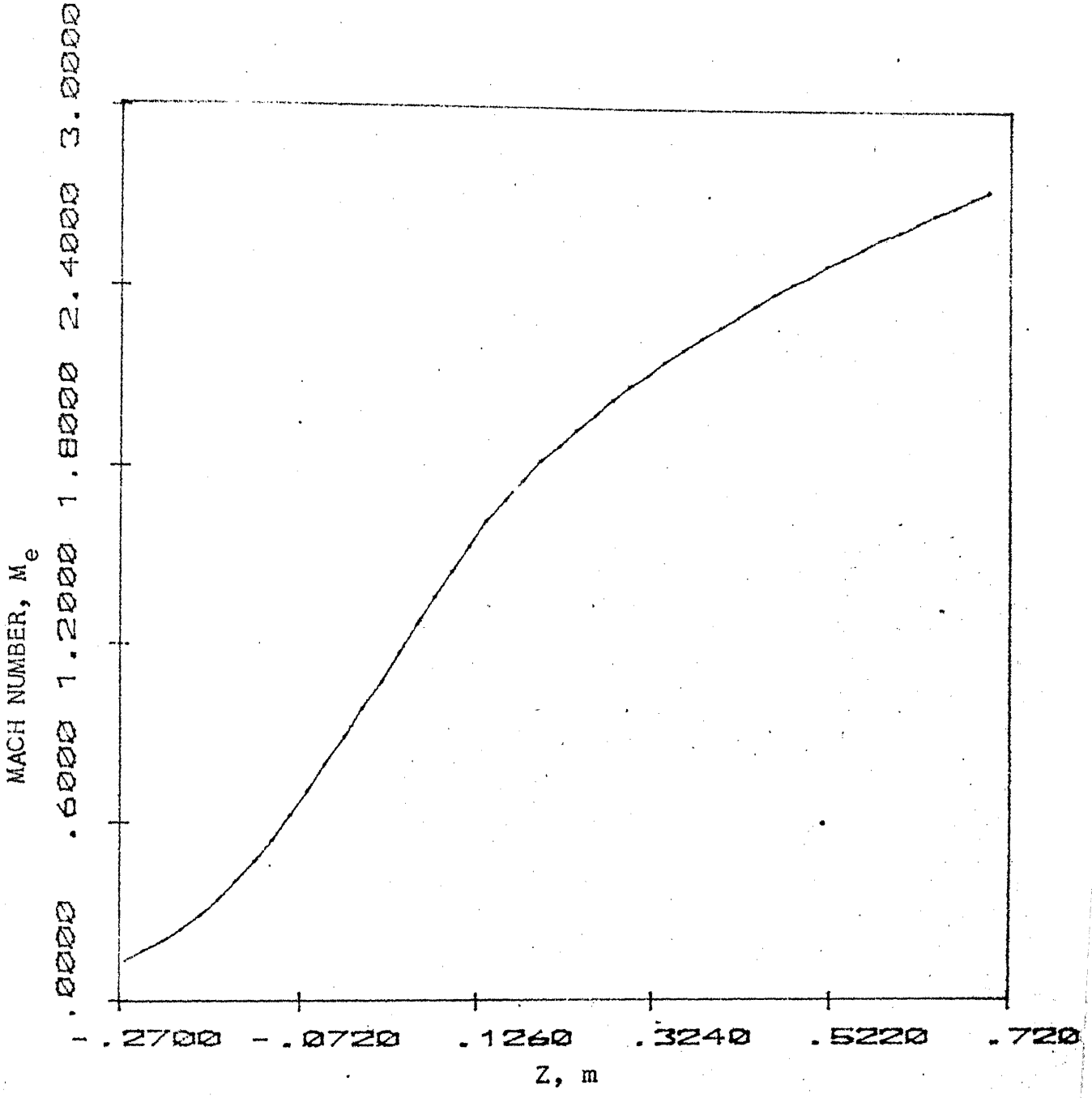

Fig. 9 Variation of Mach number along the axis of the nozzle [SLV-3].

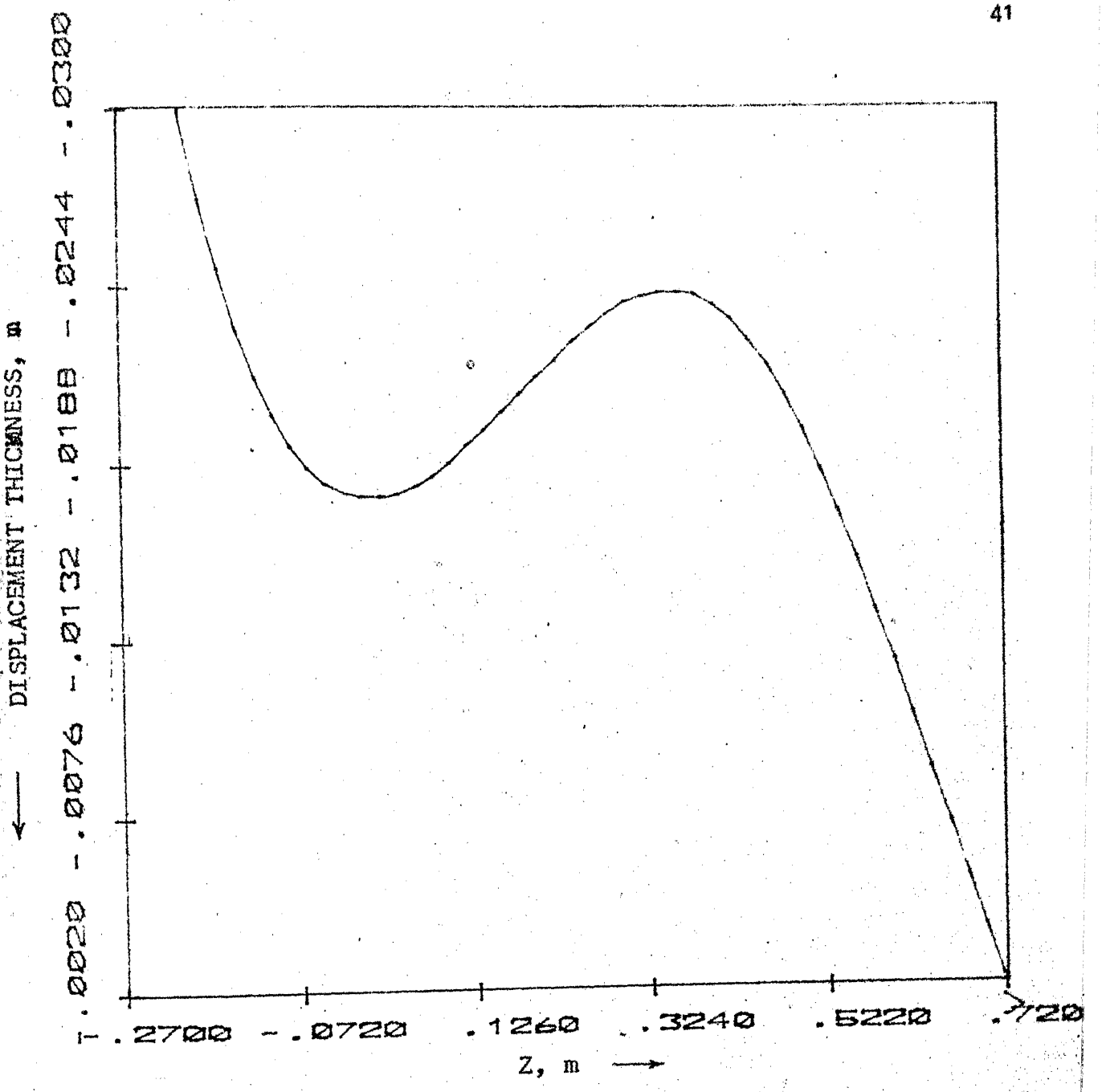

Fig. 10 Variation of Displacement thickness along the axis of the nozzle [SLV-3].

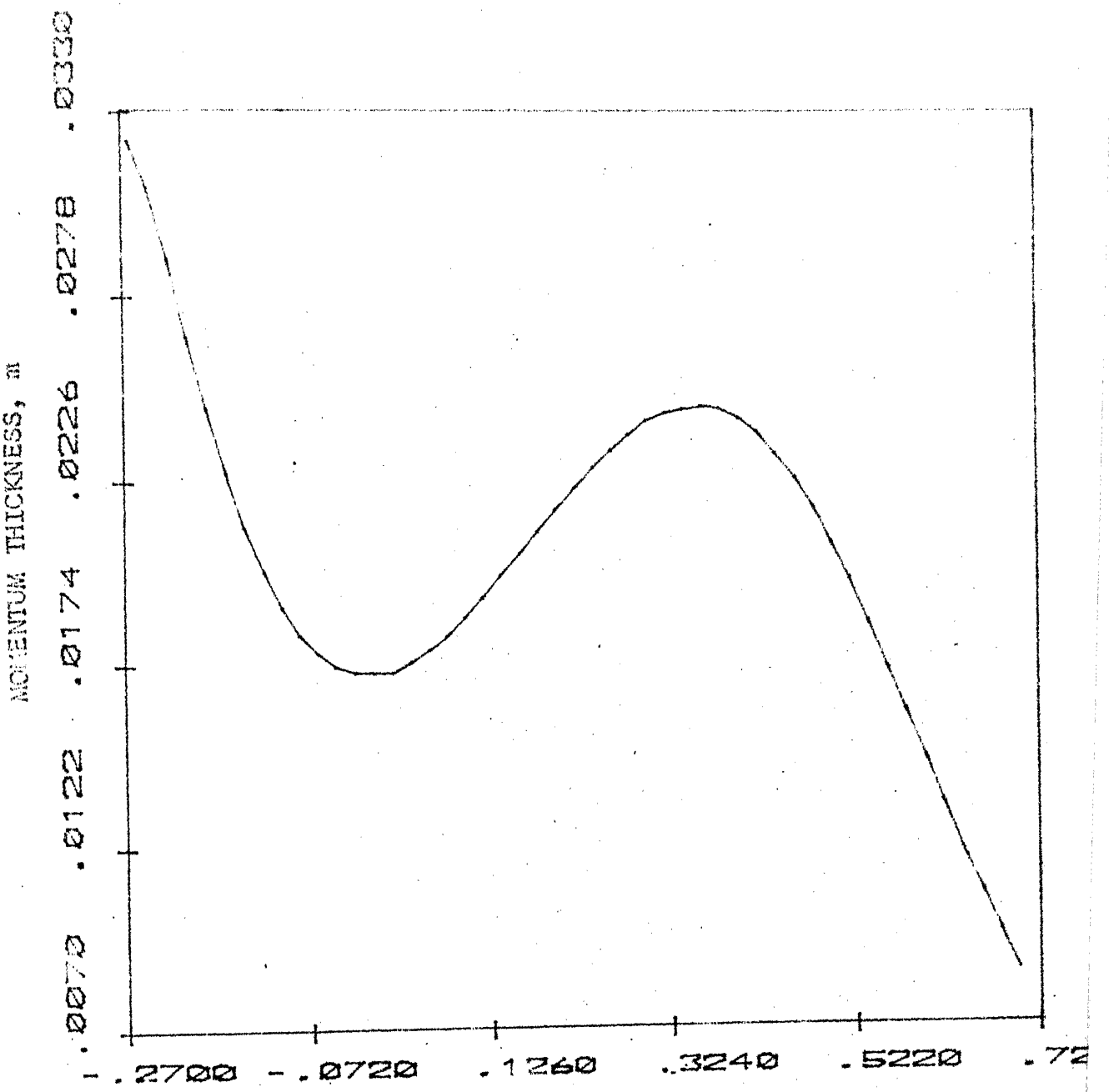

Fig. 11 Variation of momentum thickness along the nozzl
(SLV-3)

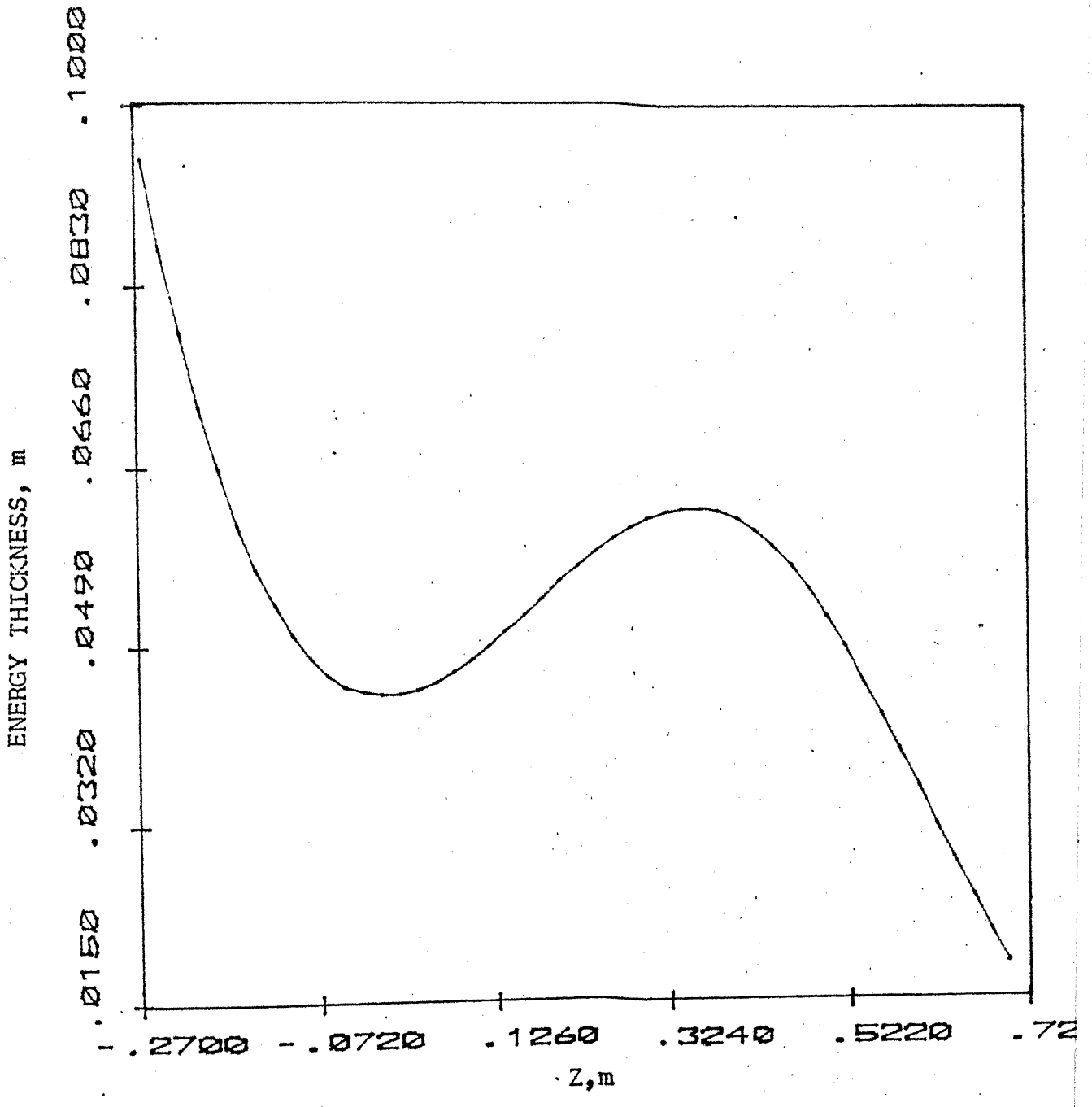

Fig. 12 Variation of energy thickness along the nozzle [SLV

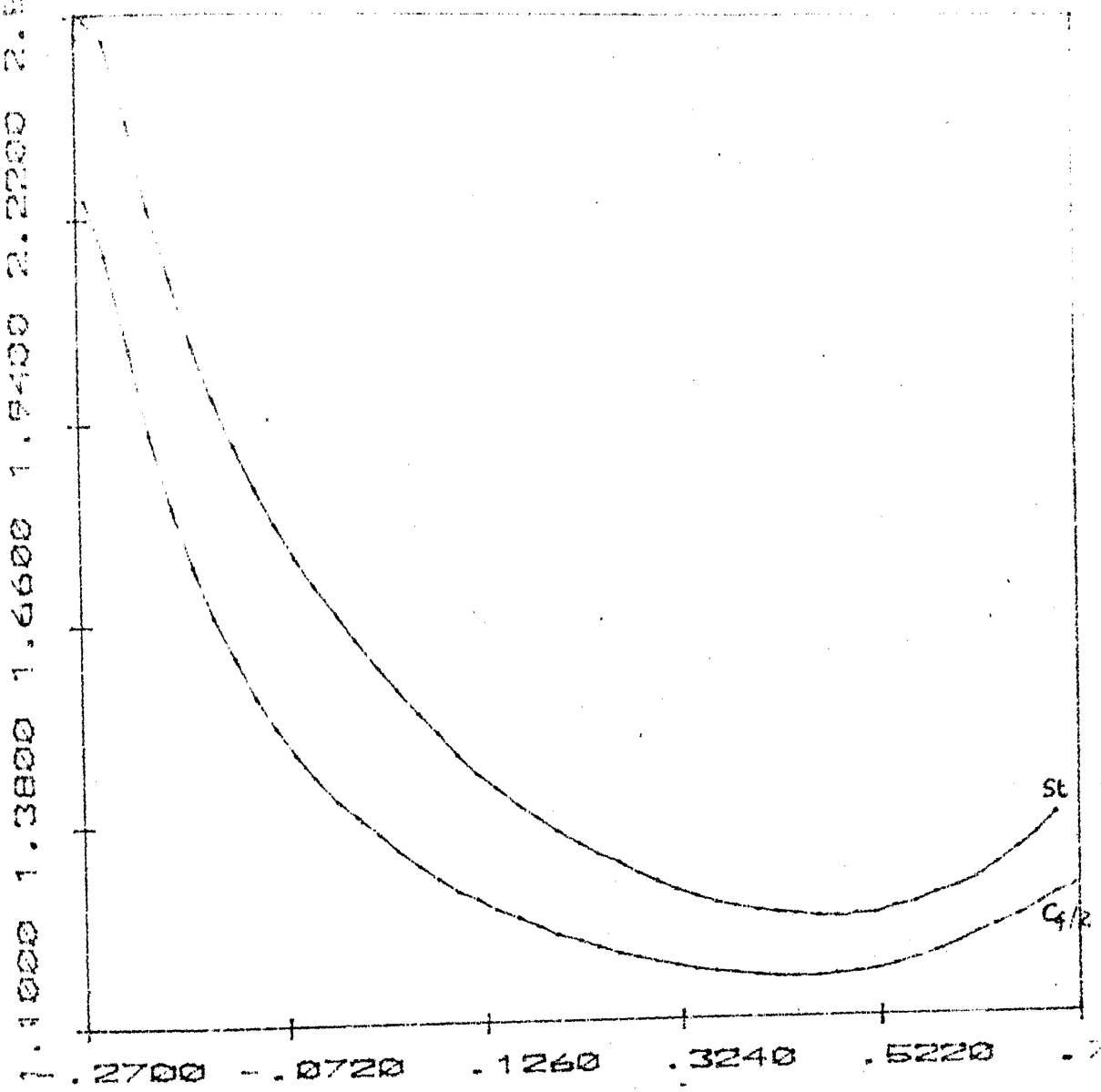

Fig. 13 Variation of $C_f/2$ and St along the nozzle [SLV-3]

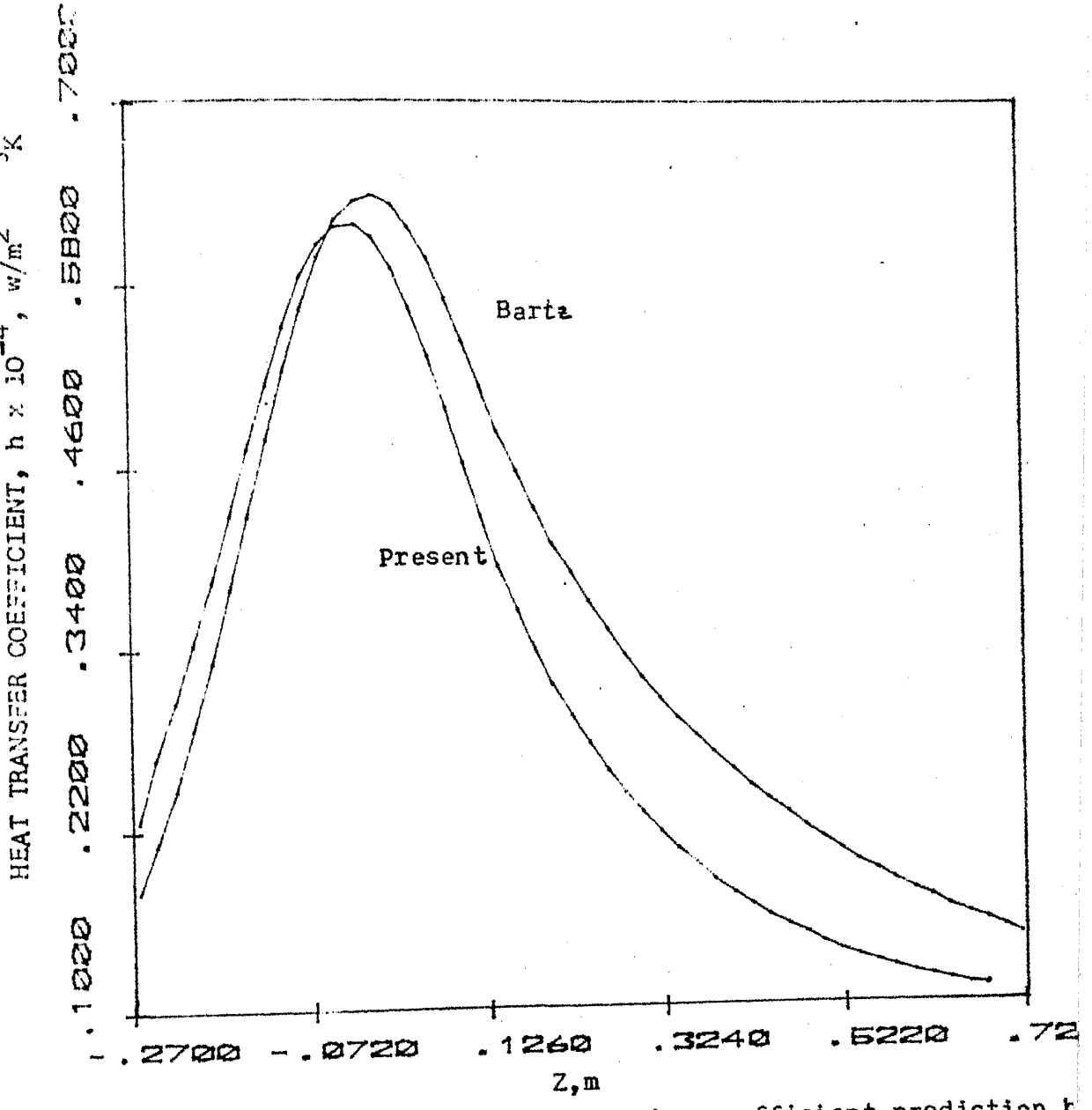

Fig. 14 Comparison of heat transfer coefficient prediction b
present method and Bartz expression

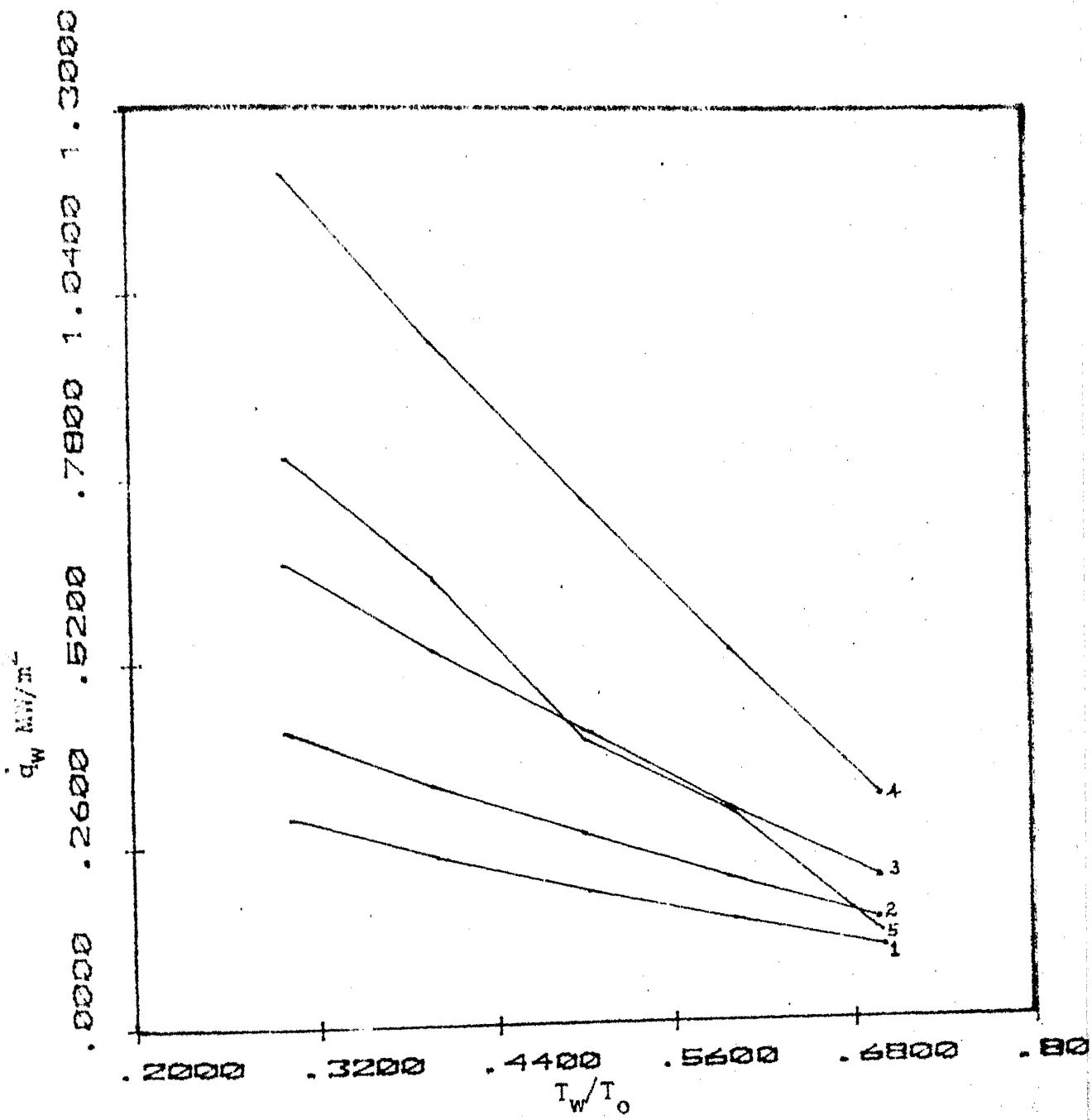

Fig. 15 Variation of heat transfer rate with wall temperatur
the convergent and throat portion of the nozzle [16]

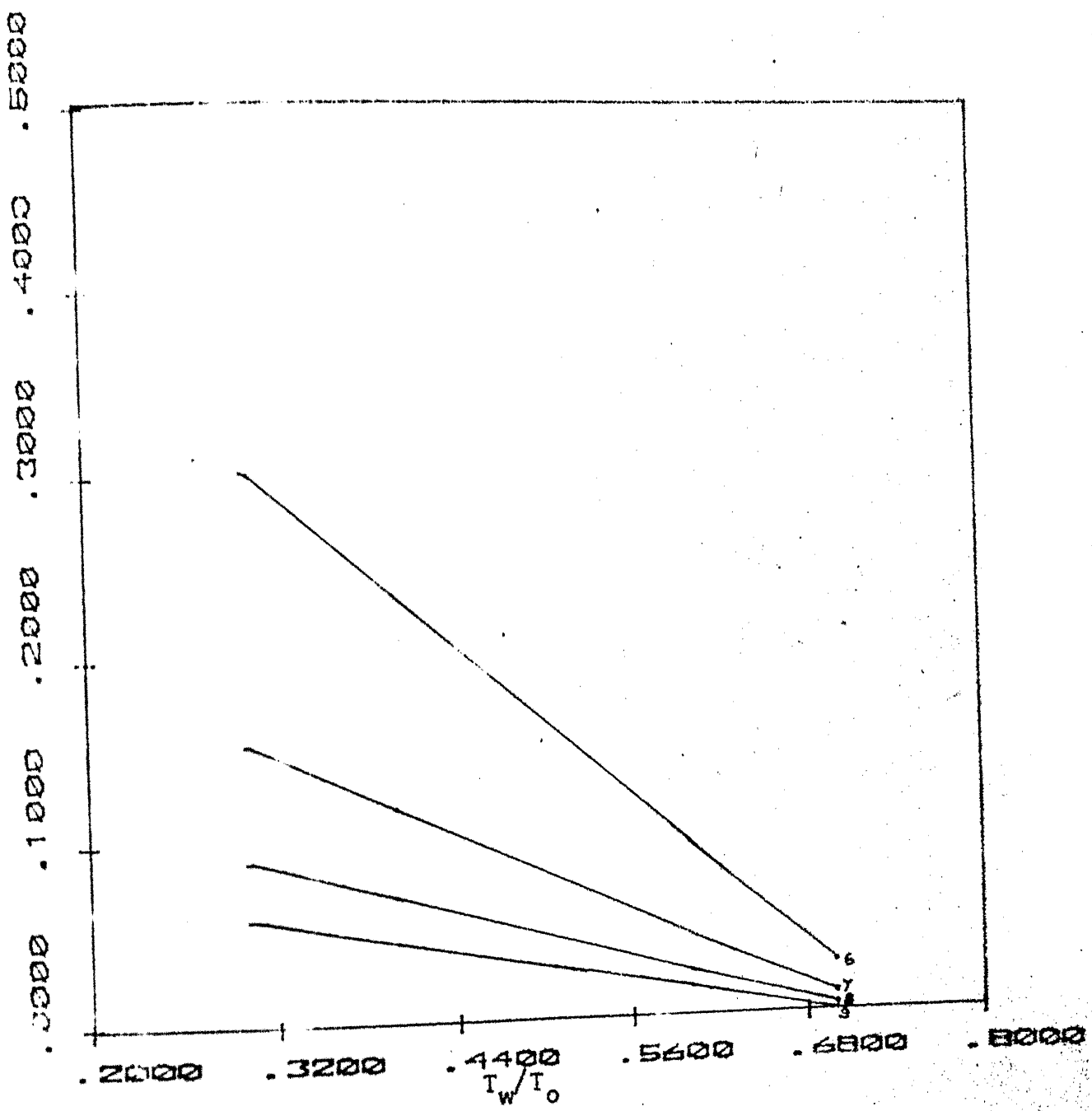

Fig. 16 Variation of heat transfer rate with wall temperature in the divergent portion of the nozzle [16]

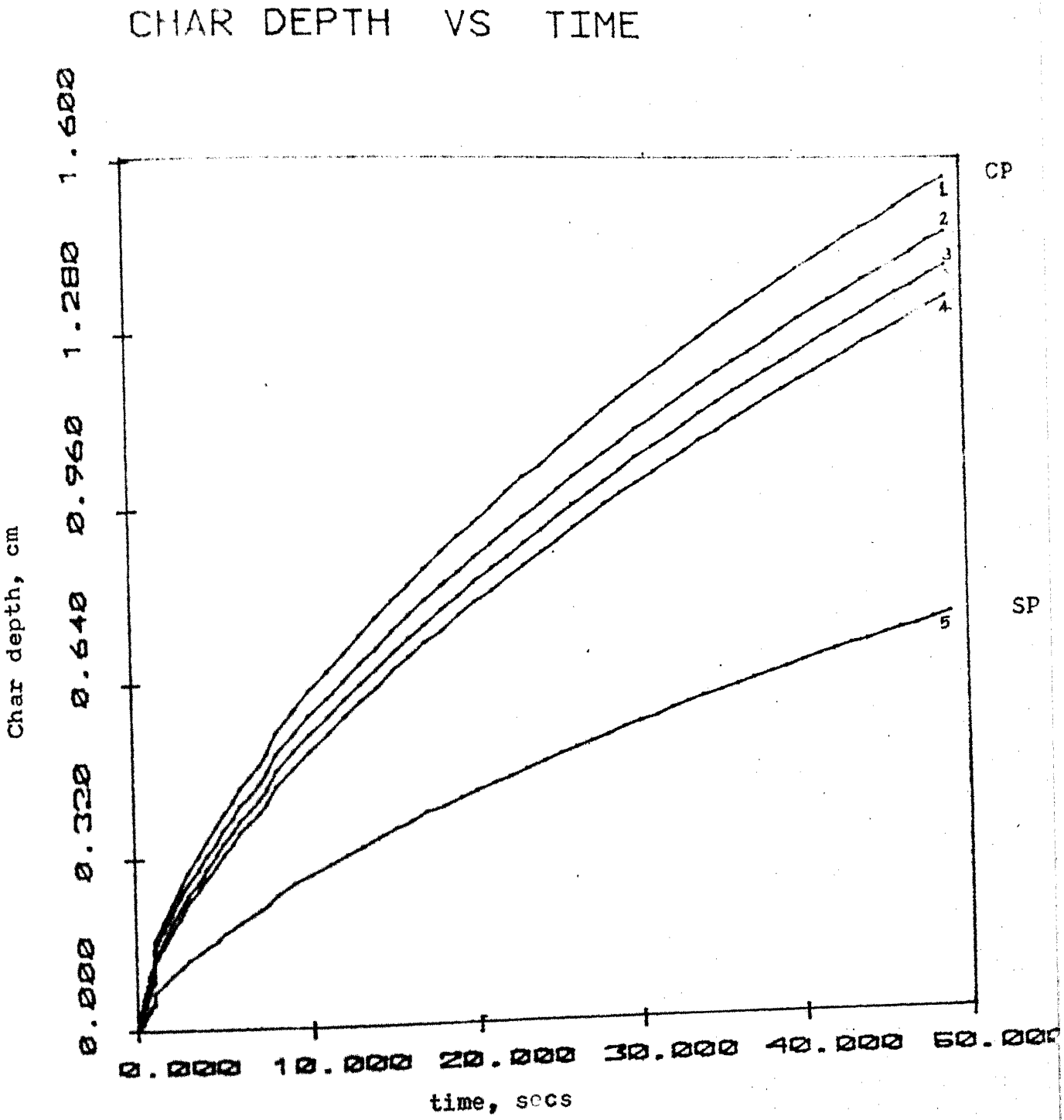

Fig. 17 Variation of char depth with time at different stations along the nozzle [SLV-3]

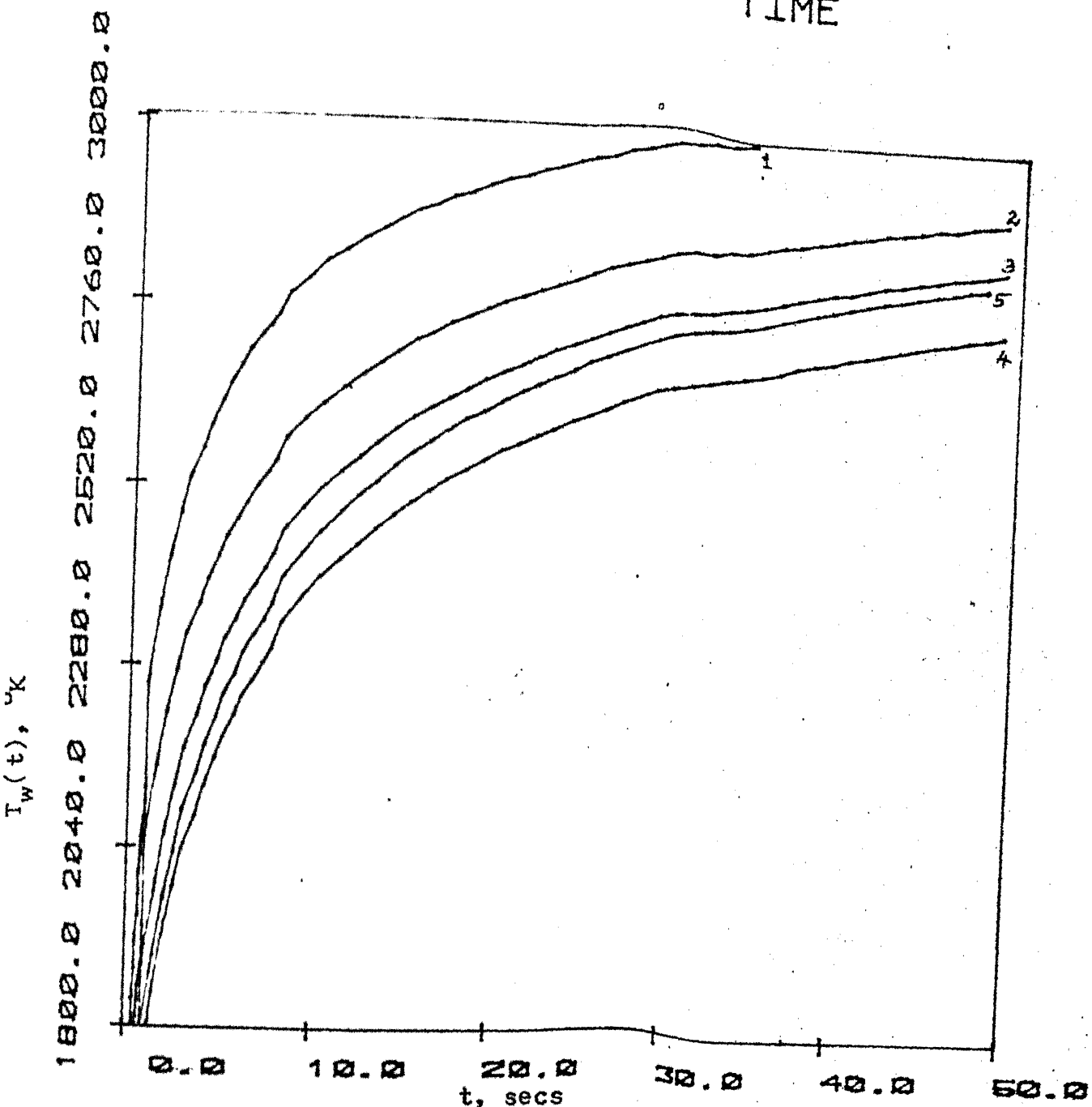

Fig. 18 Variation of surface temperature with time at different stations along the nozzle [SLV-3]. 1,2,3 and 4 for CP 5 for SP.

Table 1

Comparison of Stanton Number

Station No.	Z m	M_e	$St \times 10^3$			
			Bartz [1]	Mastanaiah [4]	Present	Expt. [16]
2	-0.1655	0.104	2.56	2.23	2.204	1.84
3	-0.127	0.137	2.493	2.177	2.10	1.775
4	-0.089	0.194	2.408	2.093	1.976	1.75
5	0.212	3.57	1.51	0.734	0.672	0.634

Table 2

Comparison of displacement thickness, momentum thickness, energy thickness and skin friction coefficient

Station No.	Z (mt)	M_e	$\delta^* \times 10^3$ (mtr)		$\theta \times 10^3$ (mtr)		$\psi \times 10^3$ (mtr)		$C_f/2 \times 10^3$	
			Expt.	Calc.	Expt.	Calc.	Expt.	Calc.	Expt.	Calc.
2	-0.1665	0.104	-0.0717	0.0694	1.195	1.186	2.54	2.43	2.66	2.218
3	-0.127	0.137	-0.303	-0.1806	0.89	0.8704	2.42	2.19	2.4	2.101
4	-0.089	0.194	-0.213	-0.295	0.76	0.643	2.03	1.907	2.3	2.216
5	0.212	3.57	-0.308	0.3998	0.965	0.952	3.00	3.066	0.88	1.03

Table 3

Data of composite liners used in the computation

A. Properties of Carbon phenolic [19]

$\rho_l = 1270$ Kg/m^3	$\rho_c = 1067$ Kg/m^3
$C_{p,l} = 1507.2$ J/Kg$^\circ$K	$C_{p,c} = 2009.6$ J/Kg$^\circ$K
$k_l = 1.14$ J/m-sec$^\circ$K	$k_c = 2.0$ J/m-sec$^\circ$K
$T_l^\circ = 330$ K	$T_p = 823$ K
$C_{p,inj} = 1670.5$ J/Kg$^\circ$K	$Q_p = 775\times10^3$ J/Kg

B. Properties of Silica Phenolic [19]

$\rho_l = 1583.0$ Kg/m^3	$\rho_c = 1327.0$ Kg/m^3
$C_{p,l} = 1256$ J/Kg$^\circ$K	$C_{p,c} = 2009.6$ J/Kg$^\circ$K
$k_l = 0.5$ J/m-sec$^\circ$K	$k_c = 0.7477$ J/m-sec$^\circ$K
$T_l^\circ = 330$ K	$T_p = 823$ K
$C_{p,inj} = 1670.5$ J/Kg$^\circ$K	$Q_p = 775\times10^3$ J/Kg

C. Thermochemical Data for C-P [20]

Equation used $\frac{\partial \rho}{\partial t} = -A \exp(-E/RT)\ \rho_o \left(\frac{\rho - \rho_r}{\rho_o}\right)^n$

$\rho_o = 1300$ Kg/m^3, $\rho_r = 770$ Kg/m^3, $n = 2$

	$T < 720$K	$T > 720$K
A sec^{-1}	0.2	1.1×10^4
E/R K	2.6×10^3	1.1×10^4

Table 4

Comparison of calculated and measured char layer thickness

Station number	Rad. mtrs	Mach number	Liner material	Char layer Thickness*, cm measured	calculated
1	0.212	1.89	CP**	1.43	1.41
2	0.230	2.06	CP**	[1.5]	1.48
3	0.26	2.29	CP**	1.2	1.24
4	0.306	2.57	SP	[1.15]	0.76
5	0.318	2.63	SP	1.10	0.76
6	0.338	2.735	SP	[1.10]	0.759
7	0.369	2.87	SP	0.8	0.69

CP - carbon phenolic

SP - silica phenolic

*Char layer thicknesses were measured at the burn out of the motor

**At this station, the carbon phenolic is backed by silica phenolic whose properties are similar as far as pyrolysis is concerned.

REFERENCES

1. Bartz, D.R., 'Turbulent boundary-layer heat transfer from rapidly accelerating flow of rocket combustion gases and of heated air', Advances in heat transfer, vol2, Edited by Hartnett, J.P. and Irvine Jr., T.P., Academic Press, New York, pp. 1-108 (1965).
2. Patanakar, S.V. and Spalding, D.B., 'Heat and mass transfer in boundary layers', Margan-Grampian Press, London (1967).
3. Cebecci, T. and Smith, A.M.O., 'Analysis of turbulent boundary layers', Academic Press, New York (1974).
4. Mastanaiah, K., 'Prediction of skin-friction and heat transfer from compressible turbulent boundary layers in rocket nozzles', Int. J. of Heat and Mass Transfer, vol. 21, 1978, pp. 1403-1409.
5. Sutton, G.W., 'The initial development of ablation heat protection: An historical perspective', J. of Spacecraft and Rocket, vol. 19, No.1, Jan-Feb, 1982, pp. 3-11.
6. Swann, R.T. and Pittman, C.M., 'Numerical analysis of the transient response of advanced thermal protection systems for atmospheric entry', NASA TND-1370,July 1962.

7. Moyer, C.B. and Rindal, R.A., 'An analysis of the coupled chemically reacting boundary layer and Charring Ablator - Part II, Finite difference solution for the in-depth response of Charring materials considering surface chemical and energy balances', NASA CR-1061, June 1968.

8. Goodman, T.R., 'Application of integral methods to transient non-linear heat transfer', Advances in heat transfer, vol.1, Academic Press, 1964, pp. 51-122.

9. Carslaw, H.S. and Jaeger, J.C., 'Conduction of heat in solids', Oxford University Press, London, 1959, p. 285.

10. Boley, B.A., 'Upper and lower bounds in problems of melting or solidifying slabs', Quart. J. Mech. Appl. Maths, vol. 17, 1964, p. 253.

11. Zien, T.F., 'Integral solution of Ablation problems with time-dependent heat flux', AIAA Journal, vol.16, No.12, December, 1978, pp. 1287-1295.

12. Zien, T.F., 'Study of heat conduction with phase transition using an integral method', AIAA Progress in Astronautics and Aeronautics, vol.56, 1977, pp. 87-111.

13. Sharma, O.P., Rotenberg, M. and Penner, S.S., 'Phase change problems with variable surface temperatures', AIAA Journal, vol.5, No.4, April 1967, pp. 677-682.

14. Shapiro, A.H., 'The dynamics and thermodynamics of compressible fluid flow', vol. I and II, Ronald Press, New York, 1954.

15. Van Driest, E.R., 'On turbulent flow near a wall', J. Aero. Sci., vol.23, 1956, p. 1007.

16. L.H. Back and R.F. Cuffel, 'Turbulent boundary layer and heat transfer measurements along a convergent-divergent nozzle, J. Heat Transfer, 93, 397, 1971.

17. Fogaroli, R.P. and Laganelli, A.L., 'Mach number and wall temperature effects on turbulent heat blockage', Progress in Astronautics and Aeronautics, vol.59, 1978, pp.156-174.

18. Gill, P.E. and Miller, G.F., 'An algorithm for the integration of unequally spaced data', The Computer Journal vol.15, No.1, Feb. 1972, pp. 80-83.

19. Private Communication: VSSC, Trivandrum.

20. Nagappa, R., Ramamurthi, K. and Muthunayagam, A.R., 'Development of a composite nozzle for a solid propellant rocket booster', Paper presented in International Astronautical Federation 30th Congress, Munich 16-23, Sept.1979.

21. Davy, W.C., Menees, G.P., Lundell, J.H. and Dickey, R.R., 'Hydrogen-helium ablation of carbonaceous materials, numerical simulation and experiment', Progress in Astronautics and Aeronautics, vol. 64 (1979), pp 228-244.

```
00100      CC        THIS PROGRAM GIVES THE HEAT TRANSFER IN NOZZLES
00200
00300                EXTERNAL FCN,MYPRGM
00400                REAL MOLWT,MACHE,MACHE1,MOMTHK,MOMTHN,MUF,MUW,MU,MUH
00500                REAL FUNC1,FUNC2,FUNC3
00600
00700
00800      CC        THIS COMMON STATEMENT IS BETWEEN THE MAIN PROGRAM AN
00900      CC        SUBROUTINE MYPRGM
01000
01100                COMMON /SHRE/MACHE,TZERO,PZERO,GAMA,R,TWBYTO,PR,ALPH
01200               1RF,F,DELTA,F1XY(2),F2XY(2),MOMTHK,ENRGTK,Z,CFB2N,ST
01300               2MOMTHN,ENRGTN,DELSTR,ADULT,AIAW,ROWEUE,DRBYDZ,XTOZ
01400
01500                DIMENSION FUNC1(155),FUNC2(155),FUNC3(155),FZERO(6),
01600                DIMENSION RCB(2),Y(2)
01700                DIMENSION C(24),W(25,9),XC(2),RC(2),RCA(2)
01800                OPEN (UNIT=12,DEVICE='DSK',FILE='NOZPLT.DAT')
01900                READ(21,*) DELSTR,MOMTHK,ENRGTK,RAD,GAMA,ST,CFBY2,PZ
02000                READ(21,*) TWBYTO,PR,MACHE,ABASTR,ALPHA,R,MOLWT,CP
02100                TYPE*,DELSTR,MOMTHK,ENRGTK,RAD,GAMA,ST,CFBY2,PZERO,T
02200                TYPE*,TWBYTO,PR,MACHE,ABASTR,ALPHA,R,MOLWT
02600      C         TO FIND THE VARIATION OF MACH NUMBER IN NOZZLE
02800
02900
03700                 AIW=CP*TW
03800                MACHE=0.1402
03900                DELSTR=-0.108;MOMTHK=0.02928;ENRGTK=0.1692
04000
04100                TEMP=TW
04400                RAD=34.0E-2
04500                RADSTR=16.5E-2
04700                PR=GAMA*4.0/(9.0*GAMA-0.5)
04900                DELTA=0.02
04900                RF=PR**0.333333
05100                Z=-26.25E-2
05200
05300                F=1.0E-6
05500                TE=TZERO/(1.0+((GAMA-1.0)/2.0)*MACHE*MACHE)
05600      999       DRBYDZ=-3.220892*3.0*Z*Z+2.0*Z*1.680642-0.356E-02
05700                XTOZ=SQRT(1.0+DRBYDZ*DRBYDZ)
05800      C          DRBYDX=(2.0*DRBYDZ/(RAD*(MACHE*MACHE-1.0)))/XTOZ
05900                IF(MACHE.EQ.1.0)DBYDX=0.0
06000                S1=DRBYDZ/RAD
06100                TAW=(1.0+RF*MACHE*MACHE*(GAMA-1.0)/2.0)*TE
```

```
06300                F1XY(1)=CFBY2*XTOZ-MOMTHK*SI*((2.0+DELSTR/MOMTHK-MAC
06400               10/(MACHE*MACHE-1.0)+1.0)
06500                F2XY(1)=SI*(TAW-TW)/(TZERO-TW)*XTOZ-ENRGTK*(-SI)
06600                S=2.0*(GAMA-1.0)/(GAMA+1.0)
06700                WRITE(12,*)Z,MACHE,DELSTR,MOMTHK,ENRGTK,CFBY2,SI,OW.
06800
06900          CC    THE MACHE NUMBER AT THE NEXT STATION IS CALCULATED BE
07100          CC    ==========================================
07200          10          Z=Z+DELTA
07300                DRBYDZ=-3.220892*3.0*Z*Z+2.0*Z*1.680642-0.356E-02
07400                XTOZ=SQRT(1.0+DRBYDZ*DRBYDZ)
07500                IF(Z.GT.14.5E-2)GO TO 1200
07600                GO TO 1400
07700          1200  RAD=19.0E-2+0.26795*(Z-14.5E-2)
07800                GO TO 1
07900          1400  IF (Z .GT.0.0)MACHE=2.0
08000          1300  RAD=-3.220892*Z*Z*Z+1.680642*Z*Z-0.356E-2*Z+16.5E-2
08100          1     ABASTR=(RAD/RADSTR)*(RAD/RADSTR)
08200                S=2.0*(GAMA-1.0)/(GAMA+1.0)
08300
08400          CC    ****
08500          CCC   IF  AREA RATIO IS LESS THAN UNITY THROAT CONDITIONS A
08600          CC    ==========================================
08700          CC    IF(ABASTR.LE.1.0)GO TO 14
08800                S1=S-1.0
08900                P=ABS(ABASTR)**S
09000                Q=S/2.0
09100                CON=+   2.0/(GAMA+1.0)
09200          11    FX=-P*((MACHE))**S+Q*MACHE*MACHE+CON
09300                F1X=-P*S*MACHE**S1+Q*2.0*MACHE
09400                MACHE1=MACHE-(FX/F1X)
09500                ERROR=(MACHE1-MACHE)/MACHE1
09600                MACHE=ABS(MACHE1)
09700                IF (ABS(ERROR).GT.E) GO TO 11
09800                TYPE*,Z,ABASTR,MACHE,RAD
09900          CC    IF THE AREA RATIO IS GREATER THE PRESCRIBED VALUE ,ST
10000          CC    ==========================================
10100                IF(ABASTR.GT.6.7) STOP
10200                GO TO 707
10300          C     APPLICABLE TO CONICAL NOZZLES ONLY ****
10400          CCC   THROAT CONDITIONS ARE GIVEN BELOW    ****
10500          C     ==========================================
10600          14    RAD=RADSTR
10700                MACHE=1.0
10800                ADULT=ABS(Z-DELTA*COS(ALPHA))/COS(ALPHA)
```

```
10900                 Z=0.0
11000                 ALPHA=0.0
11100
11200           707   CONTINUE
11300           757   FORMAT('THE ABOVE IS THE MACH NO. AT THE GIVEN Z STA
11400
11500
11600
11700           CC    2D NEWTON RALPHSON METHOD IS USED TO GET BETTER APPR
11800           C     ================================================
11900           1888  CONTINUE
12000                 XC(1)=CFRY2
12100                 XC(2)=ST
12200                 DX=1.0E-5
12300                 CALL MYPRGM(XC,RC)
12400           C     TYPE*,XC(1),XC(2),RC(1),RC(2)
12500                 NAA=1
12600           908   X=(XC(1))
12700                 XC(1)=(1.0-DX)*XC(1)
12800                 CALL MYPRGM(XC,RCA)
12900           C     TYPE*,XC(1),XC(2),RCA(1),RCA(2)
13000                 XC(1)=X
13100                 DF1X=(RC(1)-RCA(1))/(DX*XC(1))
13200                 DF2X=(RC(2)-RCA(2))/(DX*XC(1))
13300           C     TYPE*,DF1X,DF2X,RCA(1),RCA(2)
13400                 CY=(XC(2))
13500                 XC(2)=(1.0-DX)*XC(2)
13600                 CALL MYPRGM(XC,RCB)
13700           C     TYPE*,XC(1),XC(2),RCB(1),RCB(2)
13800                 XC(2)=CY
13900                 DF1Y=(RC(1)-RCB(1))/(DX*XC(2))
14000                 DF2Y=(RC(2)-RCB(2))/(DX*XC(2))
14100                 DEN=DF1X*DF2Y-DF1Y*DF2X
14200                 XC(1)=XC(1)+(RC(2)*DF1Y-RC(1)*DF2Y)/DEN
14300                 XC(2)=XC(2)+(RC(1)*DF2X-RC(2)*DF1X)/DEN
14400           C     TYPE*,XC(1),XC(2),DF1Y,DF2Y
14500                 CALL MYPRGM(XC,RC)
14600           C     TYPE*,XC(1),XC(2),RC(1),RC(2),DELTA
14800                 IF((ABS(RC(2)).LE.1.0E-6) .AND.(ABS(RC(1)).LE.1.0E-6)
15000                 IF(NAA.GT.7)  GO TO 81
                      NAA=NAA+1
                      GO TO 908

15400           CC    ITERATIONS CONVERGED WITHIN THE GIVEN ACCURACY OF STA
```

```
20700
20800
20900          COMMON /SHARE/ASTAR,A1,A2,AIW,CP,DELT,Tw,UE,UIOw
21000          DIMENSION FUNC1(155),FUNC2(155),FUNC3(155),FZERO(6),
21100         1TYPRTME(1),C(24),W(25,9),X(1),XC(2),RC(2),RCA(2)
21200         2,RCR(2)
21300    C     TYPE*,F1XY(1),F2XY(1),MOMTHK,ENRGTK
21400          POWER=GAMA/(GAMA-1.0)
21500          CFRY2=(XC(1))
21600            ST=(XC(2))
21700          TW=TWBYTO*TZERO
21800          Tw=600.0;ARASTR=(RAD/0.165)**2
21900          DELTA=0.02
22000    C     TO FIND THE FREESTREAM PROPERTIES
22100          TE=TZERO/(1.0+((GAMA-1.0)/2.0)*MACHE*MACHE)
22150          RMACHE=MACHE
22200          CP=1651.66
22300          PE=(TE/TZERO)**POWER*PZERO
22400          UE=(SQRT(GAMA*R*TE))*MACHE
22500          AIE=CP*TZERO
22600          AIW=CP*TW
22700          TNOT=TW
22800
22900          TAW=(1.0+RF*MACHE*MACHE*(GAMA-1.0)/2.0)*TE
23000          AIAW=CP*TAW
23100          TOBYTE=TZERO/TE
23200          DLMBDX=( TOBYTE*2.0*(DRBYDZ)/((MACHE*MACHE-1.0)*RAD)
23300          IF(MACHE.EQ.1.0)DLMBDX=0.0
23400          DMEBDX=DLMBDX*MACHE
23500          DTEBDX=((TE*(1.0-GAMA)*MACHE*DMEBDX)/TOBYTE)
23600          DELI=AIE-AIW
23700          DUEBDX=(2.0*DRBYDZ*UE)/(RAD*(MACHE*MACHE-1.0))
23800          IF(MACHE.EQ.1.0)DUEBDX=0.0
23900          DIBYDX=(CP*DTEBDX+UE*DUEBDX)/DELT
24000          ROWE=PE/(R*TE)
24100          ROWw=(TE/TW)*ROWE
24200          COMM=SQRT(MOLWT)*11.842E-8
24300          MUE=COMM*TE**0.6
24400          MUW=COMM*TW**0.6
24500    C     TYPE*,TZERO,TW,TE,PE,TEMP,AIE,AIW,AIAW,DMEBDX,UE,DLMB
24600
24700    C     TYPE 777
24800     777  FORMAT (5X,'TZERO,Tw,TE,      PE,TEMP,ATE,    AIW,AIAw,
24900    505   TEMP=TW
25000          TUMw=CFBY2*ROWE*UE*UE
```

```
25100             UTOW=SQRT(TOWW/ROWW)
25200     C TO FIND THE VELOCITY PROFILES IN THEBOUNDARY LAYER
25300             FUNC1(1)=1.0
25400             FUNC2(1)=0.0
25500             FUNC3(1)=0.0
25600     C
25700     C
25800      111    Y(1)=0.0
25900             X=0.0
26000             H=0.5
26100             K=2
26200             A1=ST*PR*(AIAW-AIW)/(DELT*CFBY2)
26300             AF1=((1.0-PR)*UE*UE)/(2.0*DELI)
26400     C       AF2=(CP*TW*MUW*ROWW*A1*DLMBDX)/(CP*TZERO*ROWE**2*2.*U
26500             AF2=(A1*MUW*ROWE*DUEBDX)/((CFBY2*ROWE*UE)*(CFBY2*ROWE
26600             A2=AF1+AF2+A1*A1*0.6*(TZERO-TW)/(2.0*TW)
26700     C       A2=AF1+AF2
26800     CC      TYPE*,AF2,DUEBDX,AF1,A2,A1
26900             PSTAR=((MUE/ROWE)*UE*DUEBDX)/(UTOW**3)
27000     CC      TYPE*,MUE,MUW,ROWE,UE,DUEBDX,UTOW,PSTAR,TOWW
27100     CC      TYPE 787
27200     787     FORMAT(5X,'VALUES ARE MUE,MUW,ROWE,UE,DUEBDX,UTOW')
27300             ASTAR=26.0*(1.0-11.8*PSTAR)
27350             IF(ASTAR .LT.0.0)ASTAR=0.001
27400             CDEFFT=(ROWW*UTOW)/MUW
27500     C       TYPE*,ASTAR,CDEFFT
27600     404     CONTINUE
27700             AYSTAR=Y(1)
27800     77      ROW=(TW/TEMP)*ROWW
27900             MU=CONM*TEMP**0.6
28000             MUBMUW=MU/MUW
28100             ROBROW=TW/TEMP
28200             B=MUBMUW*MUBMUW
28300
28400             IF((X*UTOW).GE.(0.99*UE)) GO TO 100
28500             IF((X*UTOW).GE.(0.9*UE)) H=0.1
28600             TOL=1.0E-4
28700             NW=25
28800             IND=1
28900             XEND=X+H
29000             M=1
29100
29200
29300
29400
29500
```

```
      CALL DVERK(N,FCN,X,Y,XEND,TOL,IND,C,NW,W,IER)
C       TYPE*,Y,Y(N),B,DMPFN


        U=X*UTOW
        AY(K)=Y(N)/COEFFT
        PHI=U/UE
        AISTR=A1*PHI+A2*PHI*PHI
        AI=ATSTR*DELT+AIW
        TEMP=(A1-(U*U/2.0))/CP
        TNOT=TEMP+(U*U)/(2.0*CP)
C       TYPE *,AY(K),U,TEMP,AISTR,PHI,TNOT,ROW
797     FORMAT (F12.7,5X,F6.3,3X,F7.3, 5X,F6.4,5X,F7.3 ,5X,F
902     CONTINUE
        ROW=(TW/TEMP)*ROWW
        ROWU=ROW*U
        ROWEUE=ROWE*UE
        COMTRM=ROWU/(ROWE*UE)
C       TYPE*,ROW,U,ROWU,ROWE,UE
        FUNC1(K)=(1.0-COMTRM)
C       IF(COMTRM.GT.1.0) FUNC1(K)=0.0
        FUNC2(K)=(1.0-PHI)*COMTRM
        FUNC3(K)=(1.0-AISTR)*COMTRM
C       TYPE*,ROW,COMTRM,FUNC1(K),FUNC2(K),FUNC3(K),PHI,AISTR
        K=K+1
C         IF(TNOT.GE.800) GO TO 100
        GO TO 404
C       ================================================
C       NUMERICAL INTEGRATION USING NAG ROUTINE FOR BOUNDARY
CC      INTEGRAL PARAMETERS
CC      ================================================
100     IFAIL = 0
C       INTEGRATION FOR DISPLACEMENT THICKNESS
        K =K-1
        CALL D01GAF(AY,FUNC1,K,ANS,ER,IFAIL)
        SUM1=ANS

C               INTEGRATION FOR MOMENTUM THICKNESS


        IFAIL = 0
        CALL D01GAF(AY,FUNC2,K,ANS,ER,IFAIL)
```

```
34000                 SUM2=ANS
34100
34200       C                 INTEGRATION FOR ENERGY THICKNESS
34300
34400                 TRAIL = 0
34500       C          TYPE*,ER
34600                 CALL DQICAF(AY,FUNC3,K,ANS,ER,TRAIL)
34700                 SUM3=ANS
34800
34900
35000                 DELSTR=SUM1
35100                 MOMTHN=SUM2
35200                 ENRGTN=SUM3
35300
35400       C         TYPE *,DELSTR,MOMTHN,ENRGTN,ROWE,UE,RAD,TAW,TW
35500       757       FORMAT (5X,'DELSTR',5X,'MOMTHK',5X,'ENRGTK')
35600       C         TYPE 757
35700       CCC
35800       C
35900                 SI=DRBYDZ/RAD
36100                 DTHETA=(MOMTHN-MOMTHK)/DELTA*2.0
36200                 DPSI=(ENRGTN-ENRGTK)/DELTA*2.0
36300                 DBYUDX=(2.0*DRBYDZ/(RAD*(MACHE*MACHE-1.0)))/XTOZ
36400                 IF(MACHE.EQ.1.0)DBYUDX=0.0
36700                 F1XY(2)=MOMTHK*SI*((2.0+DELSTR/MOMTHK-MACHE*MACHE)*2.
36800                 10/(MACHE*MACHE-1.0)+1.0)
36900                 F2XY(2)=ENRGTK*(-SI)
37000                 DIMTEM=(TAW-TW)/(TZERO-TW)
37100
37200
37300
37400                 CFB2N=(DTHETA-F1XY(1)+F1XY(2))/XTOZ
37500                 STTEMP=(DPSI-F2XY(1)+F2XY(2))/XTOZ
37600                 STNEW=STTEMP/DIMTEM
37700                 STNEW=STNEW
37800
38000
38100                 ERCF=(CFB2N-CFBY2)/CFB2N
38200                 ERST=(STNEW-ST)/STNEW
38300       C         TYPE*,CFBY2,CFB2N,ST,STNEW,F1XY(1),F1XY(2),F2XY(1),F2
38400       C         TYPE*,SI,DTHETA,DPSI,DBYUDX,DIMTEM,STTEMP
38500                 PC(1)=(CFB2N)-CFBY2
38600
38700                 PC(2)=(STNEW)-ST
38800       C         TYPE*,DTHETA,DPST,ERCF,ERST,SI,DBYUDX
```

```
38800 C          TYPE*,Z,CFR12,SI
38900            RETURN
39000            END
39100
39200
39300
39400
39500 C=======================================================
39600 C=======================================================
39700            SUBROUTINE FCN(N,X,Y,YPRIME)
39800            COMMON /SHARE/ASTAR,A1,A2,AIW,CP,DELT,TW,UE,UTOW,
39900            DIMENSION Y(N),YPRIME(N)
40000            AAAX=X*UTOW
40100            PHI=AAAX/UE
40200            AISTAR=A1*PHI+A2*PHI*PHI
40300            AI=AISTAR*DELI+AIW
40400            TEMP=(AI-AAAX*AAAX/2.0)/CP
40500            ROBROW=(TW/TEMP)
40600            B=(TEMP/TW)**1.2
40700            D=1.0/EXP(Y(N)/ASTAR)
40800            DMPFN=1.0-D
40900
41000            SUBFN=SQRT(B+4.0*ROBROW*0.16*Y(N)*Y(N)*DMPFN*DMPFN)
41100
41200            YPRIME(N)=0.5*(SQRT(B)+SUBFN)
41300
41400
41500
41600
41700            RETURN
41800            END
41900 C
42000 C
42100 C=======================================================
42200 C=======================================================
42300 C=======================================================
```

```
00112      C     ================================================================
00118      C                                CHAR.FOR
00121      C     ================================================================
00123      C     THIS PROGRAM CALCULATES THE CHAR LAYER THICKNESS
00125      C     AS WELL AS THE SURFACE TEMP OF ACHARRING ABLATOR
00150      C     ================================================================
00200      C     THE SUBROUTINE ARR CALCULATES  THE RATE  AT WHICH DE
00225      C      GASES ARE COMING OUT
00250      C     SUBROUTINE ARRR CALCULATES THE BLOCKING EFFECT
00300            DIMENSION AYY(30),DROBYI(30)
00400            COMMON QDOT
00500      C     GIVE THE INPUT DATA FROM HEAT TRANSFER ANALYSIS
00600
00800            TAW=3220.0;AH=2580.0
00850      C     HERE GIVE THE MATERIAL PROPERTIES
00900            CPVIR=1507.2;ROCHAR=1067.0;ROWVIR=1270.0;TINF=330.0
01000            CHARK=2.0;TPABL=2173.0;CPCHAR=2009.6;TP=823.0;VIRK=1
01100            QLP=775000.0;TZERO=3300.0;QABL=144.0E+5
01150      C     ----------------------------------------------------------------
01200            TIME=0.0;DTIME=0.00001
01300            QZERO1=AH*(TZERO-TINF)
01400            QZERO2=AH*(TZERO-TP)
01500            QZERO=(QZERO1+QZERO2)/2.0
01600            ALPHA1=CHARK/(ROWVIR*CPCHAR)
01700            ALPHA2=VIRK/(ROWVIR*CPVIR)
01800            TIM=VIRK*(TP-TINF)/(QZERO1*1.128*SQRT(ALPHA1))
01900            TIME1=TIM*TIM
02100            TIM=VIRK*(TP-TINF)/(QZERO2*1.128*SQRT(ALPHA1))
02200            TIME2=TIM*TIM
02400
02500            TIM=VIRK*(TP-TINF)/(QZERO*1.128*SQRT(ALPHA1))
02600            TIME=TIM*TIM
02700
02900      C     TYPE *,TIME1,TIME2,TIME
03100            TNOT=820.0;DTIME=0.05;CHARD=0.0
03400            AA=CHARK/(2.0*QLP*ROWVIR*ALPHA1)
03500            BB=CHARK/(QLP*ROWVIR)
03600            CC=(VIRK*(TP-TINF))/(QLP*ROWVIR*SQRT(3.1416*ALPHA2))
03700
03800
03900      C     HERE GIVE THE DATA FROM THE HEAT TRANSFER PROGRAM
04000            AH2170=2665.0;AH823=3438.05
04100            AIMOT=830.0;ACHARD=1.0E-6
04600      707   TIME=TIME+DTIME
04700            IF(ATNOT .EQ.830.0)GO TO 99
```

```
                ATNOT=TNOT+20.0;ACHARD=CHARD+1.0E-5
   99           CONTINUE
C
C               IF(TIME.GT.0.05)DTIME=DTIME*10.0
C                IF(TIME.GT.0.1)DTIME=0.05
                IF(TIME.GT.1.0)DTIME=0.5
                IF(TIME.GT.8.0)DTIME=1.0
C                PART10=AH*TAW*ACHARD+CHARK*TP+TNOT*ACHARD*ACHARD/(2
     1*CHARK/DTIME
                PART10=(AH823+(TNOT-823.0)*(AH2170-AH823)/(1800.0-82
     1ACHARD*TNOT/(2.0*ALPHA1*DTIME)+CHARK*TP/ACHARD
                PART11=CHARK/ACHARD+ACHARD/(2.0*ALPHA1*DTIME)+(AH823
     1823.0)*(AH2170-AH823)/(1800.0-823.0))
                ATNOT=PART10/PART11


                AAA=(1.0/DTIME+AA*(ATNOT-TNOT)/DTIME)
                BBB=(CC/SQRT(TIME)-CHARD/DTIME)

                CCC=-BB*(ATNOT-TP)

                .

                PART12=BBB*BBB-4.0*AAA*CCC
                IF(PART12.LT.0.0)STOP
                ACHARD=(-BBB+SQRT(PART12))/(2.*AAA)
                IF(TIME .GT. 51.0)GO TO 123
                IF(ABS((ACHARD-OLD1)/ACHARD).LT. 1.0E-6)GO TO 888
                OLD1=ACHARD;OLD2=ATNOT
                GO TO 99
  888           RAM=(ACHARD-CHARD)/DTIME
  808           TNOT=ATNOT;CHARD=ACHARD
                QDOT=(AH823+(TNOT-823.)*(AH2170-AH823)/(1800.-823.))*
                TYPE *,TIME,CHARD,TNOT
                GO TO 707
  123           CONTINUE
 1234           FORMAT(5x,'BLOCKING EFFECT IS CALCULATED BELOW')
C               CALL ARR(CHARD,ALPHA2,RAM,ROVW)
C                       ROWEUE=921.0      ;TW=2170.       ;      AMACHE=
C                       CALL  ARRR(ROVW,ROWEUE,TW,AH,AMACHE,AH1)
                STOP
                END
C               ================================================F===
C  MASS FLOW _I_r TO THE ABLATING SURFACE
```

```
C       ARRHENIUS EQUATION IS USED
C       ==========================================================
        SUBROUTINE ARR(CHARD,ALPHA2,RAM,ROVW)
        DIMENSION AYY(50),DROBYT(50)
        COMMON QDOT
        TPL=1073.0;TP=690.0;TEMP=TPL+20.0;N=1;TPABL=2170.0;
        CHARK=1.5
        ADEL=RAM/ALPHA2
5       TEMP=TEMP-20.0
        AY=ALOG((TEMP-TINF)/(TPABL-TINF))/ADEL

        AYY(N)=CHARD-AY


        IF(TEMP .GT.720.0) GO TO 1
        IF(TEMP .LE. 720.0) GO TO 2
1       A=1.1E+4;EBYR=1.1E+4
        GO TO 3
2       A=0.2;EBYR=2.6E+3

3       ROZERO=1900.0;ROWR=770.0;INDEX=2
C       USING A LINEAR VARIATION OF DENSITY WITH TEMP FROM V


        ROW=(ROWR-ROZERO)*(TEMP-TP)/(TPL-TP)+ROZERO

        DROBYT(N)=ABS(-A*EXP(-EBYR/TEMP)*ROZERO*((ROW-ROWR)/
       1INDEX)
C        ABS VALUE IS TAKEN BECAUSE THE DENSITY IS DECREASING
        N=N+1
        IF(TEMP.LE.TP)GO TO 4
        GO TO 5

4       IFAIL=0;NEW=N-1
        CALL D01GAF(AYY,DROBYT,NEW,ANS,ER,IFAIL)
        CONTINUE

C       IF CHAR REMOVAL IS TAKING PLACE USE THE EQUATION BELO
C       REMCHR=QZERO/QLABL*(ANEWC*(3.0-2.0/DEL)/(1.0+ANEWC))
        ROVW=ANS+REMCHR
```

```
15700
15800                 RETURN
15900                 END
16000       C         ================================================*===*
16100
16200
16300
16400
16500
16600       C         ================================================*====
16700       CCC       THIS IS THE SUBROUTINE FOR  FINDING OUT THE BLOCKING
16800       CCC       EFFECT DUE TO THE PYROLYSIS GASES
16900
17000                 SUBROUTINE ARRR(ROVW,ROWEUE,TW,AH,AMACHE,AH1)
17100                 TAW=3200.0
17200                 CPINJ=1670.5;CPAIR=1651.66;STNOT=AH/(ROWEUE*CPAIR)
17300                 TZERO=3300.0
17400                 TE=TZERO/(1.+0.125*AMACHE*AMACHE)
17500                 BLAMDA=ROVW/ROWEUE
17600                 APART=(TW/TE)**(1.0/8.0)
17700                 OMEGA=1.0/APART+AMACHE/8.0
17800                 BH=(CPINJ/CPAIR)*(BLAMDA/STNOT)
17900                 BCR=EXP(1.676*(OMEGA+0.161))
18000                 STCOR=(1.0-(BH/BCR))**(2.6*OMEGA)*STNOT
18100                 OCOR=STCOR*ROWEUE*(TAW-TZERO)
18200       C
18300                 AH1=STCOR*ROWEUE*CPAIR
18500
18900                 RETURN
19200                 END
19900
19100       C         ================================================*====
19200       C         ================================================*====
```